AIMS Mathematics, 11(10): 35655–35697.
DOI: 10.3934/math.20261382
Received: 17 July 2026
Revised: 14 October 2026
Accepted: 19 October 2026
Published: 30 October 2026

http://www.aimspress.com/journal/Math

Research article

Threshold dynamics of a distributed-delay SEIR model for avian influenza transmission in bird populations

Mohammed H. Alharbi*

Department of Mathematics and Statistics, College of Science, University of Jeddah, Jeddah, Saudi Arabia

* **Correspondence:** Email: mhhalharbi1@uj.edu.sa.

Abstract: Avian influenza persists as an infectious threat across wild and domestic bird populations. This paper develops deterministic SEIR models to study avian influenza transmission in a bird population. We first formulate a non-delayed model with a general saturated incidence function and derive the basic reproduction number ($\mathcal{R}_0$). The analysis shows that the disease-free equilibrium is locally and globally asymptotically stable when $\mathcal{R}_0 \leq 1$. When $\mathcal{R}_0 > 1$, a unique endemic equilibrium exists and is locally and globally asymptotically stable. The model is then extended by including three distributed-time delays that describe the delayed transition into the exposed, infectious, and recovered classes. This delayed formulation reflects variability in latency, infectious progression, and recovery among infected birds. The delayed model is shown to be mathematically well posed through the non-negativity and boundedness of its solutions. The delayed reproduction number ($\mathcal{R}_d$) is derived, and suitable Lyapunov functionals are constructed to establish the global threshold dynamics. In particular, the disease-free equilibrium is globally asymptotically stable when $\mathcal{R}_d \leq 1$, whereas the endemic equilibrium is globally asymptotically stable when $\mathcal{R}_d > 1$. Numerical simulations support the theoretical results and show how distributed delays affect the persistence of avian influenza in the bird population. Sensitivity analysis identifies the parameters that have the strongest influence on $\mathcal{R}_d$. In addition, the control simulations indicate that sufficiently strong transmission-blocking measures can reduce $\mathcal{R}_d$ and shift the system from endemic persistence to disease elimination.

Keywords: avian influenza; SEIR model; distributed delay; saturated incidence; global stability; Lyapunov functional; basic reproduction number
Mathematics Subject Classification: 92D30, 34K20, 34K60, 34D20, 37N25, 34D05

1. Introduction

Avian influenza persists as an infectious threat across wild and domestic bird populations [1–3]. Wild aquatic birds sustain the virus as a natural reservoir, while outbreaks in poultry cause severe production losses [1, 4]. The disease also carries consequences for wildlife conservation and, through spillover to mammals, for public health [3, 5, 6]. The causative influenza A viruses are naturally maintained in wild aquatic birds and may be introduced into domestic poultry through migration, environmental contamination, or direct and indirect contact with infected birds [1, 5, 7]. Their clinical impact varies widely: Low-pathogenic strains may cause mild or limited clinical disease, whereas highly pathogenic strains can spread rapidly, produce severe illness and high mortality, and generate substantial economic losses [2, 4].

Control of avian influenza is difficult because transmission is not driven by a single pathway. Wild birds can serve as natural reservoirs of avian influenza viruses [7]. Domestic birds may then amplify the infection once the virus enters poultry populations. Contaminated environments can also maintain exposure risks over time and across different locations [1, 4]. Control is further complicated by the absence of a broadly applied vaccination strategy that protects the full range of susceptible avian hosts. This limitation is especially relevant for wild birds and many non-commercial bird populations [8–10]. Control therefore depends on non-pharmaceutical measures whose effectiveness must be compared: surveillance and biosecurity to limit introduction, and movement restrictions, quarantine, and removal of infected or exposed birds to contain established outbreaks [4, 8, 11]. These features make mathematical modeling useful, not simply as a descriptive tool, but as a way to connect biological assumptions with threshold quantities that determine whether infection dies out or persists.

Mathematical models have long been used to study how avian influenza spreads and how it might be contained. Mechanistic models in particular link biological assumptions to quantities that can be measured or estimated: transmission rates, outbreak size, and the thresholds that separate persistence from extinction. Working within this framework, earlier studies have estimated transmission parameters, weighed competing intervention strategies, and assessed how culling, vaccination, surveillance, and movement restrictions shape outbreak dynamics [12]. For instance, Pandit et al. [13] used a stochastic model to study highly pathogenic H5N1 transmission between wild birds and domestic poultry in West Bengal, India, and showed that repeated introduction from wild birds together with poultry-level transmission can sustain outbreak risk. Tuncer and Martcheva [14] examined seasonal H5N1 dynamics and found that periodic bird-to-bird transmission can reproduce observed seasonal patterns. Kang et al. [15] incorporated time delays and control measures into an avian influenza model and investigated how slaughtering, education, and treatment affect disease burden.

Despite these contributions, many avian influenza models still represent the transition from exposure to infectiousness by a constant progression rate or by a single fixed delay. This assumption is biologically restrictive, since infected birds do not all share the same latent period: Its length varies with host species, viral strain, infecting dose, and environmental conditions, ranging from a few days in an individual bird to as long as two weeks within a flock [16, 17]. A constant rate is particularly limiting, as it forces an exponentially distributed latent period and thereby assigns the greatest probability to an almost immediate transition, at odds with the very notion of an incubation period. A further simplification is that birds may die during the latent or infectious stages before progressing, so that

only a fraction of an exposed cohort ever becomes infectious. Replacing a single transition time by a distribution of transition times, together with an explicit survival factor, therefore offers a more realistic description of infection development in bird populations.

Motivated by this limitation, we formulate a distributed-delay SEIR model for avian influenza transmission in a single bird population. Infection is described by a general saturated incidence function, so that the force of infection levels off at high densities of infectious birds rather than growing without bound. To represent variability in the timing of disease progression, the model incorporates three distributed-delay kernels $\zeta_i(\tau)$, $i = 1, 2, 3$, which weight the times required for birds to enter the exposed, infectious, and recovered classes [18–21]. Because a bird may die or be removed before completing any of these transitions, we attach to each kernel a survival factor and define the survival-weighted kernels

$$\Pi_i(\tau) = \zeta_i(\tau)\, e^{-n_i\tau}, \qquad i = 1, 2, 3,$$

in which $e^{-n_i\tau}$ is the probability that a bird survives a delay of length τ at the per-capita mortality rate n_i.

The novelty of this work is twofold. First, from a *modeling perspective*, we formulate an SEIR model that combines a general saturated incidence function with three distributed-delay kernels and survival factors. This structure captures realistic variability in the timing of disease progression while explicitly accounting for mortality during the delayed stages. Second, from an *analytical perspective*, we establish global threshold dynamics for both the non-delayed and delayed systems. For the distributed-delay model, we construct suitable Lyapunov functionals to prove that the disease-free equilibrium is globally asymptotically stable when the delayed reproduction number does not exceed one, and that a unique endemic equilibrium is globally asymptotically stable when it exceeds one. The survival-weighted delay terms make explicit how variability in the latent period enters the basic reproduction number; numerical simulations then illustrate the dynamical consequences of this dependence and identify the parameters that most strongly determine whether avian influenza dies out or persists in the bird population.

The paper is organized as follows. Section 2 introduces the model formulation and states the main assumptions. Section 3 analyzes the corresponding non-delayed model. Section 4 treats the distributed-delay model and its global threshold behavior. Section 5 presents numerical simulations together with a sensitivity analysis of $\mathcal{R}_d$. Section 6 concludes with the main findings, limitations, and directions for future work.

2. Model development

The bird population under consideration is divided into four epidemiological classes: susceptible birds, exposed birds, infectious birds, and recovered birds, denoted by $S(t)$, $E(t)$, $I(t)$, and $R(t)$, respectively. Susceptible birds are those that have not yet acquired avian influenza but may become infected after effective contact with infectious birds. Once infection occurs, birds do not necessarily become infectious immediately. Instead, they may pass through a latent stage during which the virus is developing within the host, but the bird has not yet reached the level of infectiousness required to contribute effectively to transmission. This justifies the inclusion of the exposed class, $E(t)$, which represents infected birds that are not yet infectious. The infectious class, $I(t)$, consists of birds that are capable of transmitting avian influenza to other susceptible birds. Although infectiousness may vary

among infected birds due to differences in viral shedding, host species, virus strain, and environmental conditions, the present model represents all infectious birds within a single compartment in order to keep the transmission structure analytically tractable. After infection, several epidemiological outcomes are possible. An infectious bird may die as a result of disease-induced mortality, recover from infection and move to the recovered class, or be removed from effective contact with the population through control measures such as isolation or culling. In this study, recovered birds are assumed to acquire immunity and are not considered susceptible to reinfection during the time scale of the model.

Compartmental models provide a convenient framework for describing how the number of birds in each epidemiological class changes over time. Throughout this study, the same symbol used to denote a compartment also represents the number of birds in that compartment. The parameter Λ denotes the recruitment rate of susceptible birds due to hatching, birth, or immigration into the population. ψ represents the saturated incidence rate, which describes the effective transmission of avian influenza from infectious birds to susceptible birds when contact becomes limited at high infection levels. ε denotes the progression rate at which exposed birds leave the latent class and become infectious, while γ represents the recovery rate of infectious birds. Moreover, μ_s, μ_e, μ_i, and μ_r denote the natural mortality rates of susceptible, exposed, infectious, and recovered birds, respectively.

For notational convenience, we define $(S, E, I, R) = (S, E, I, R)(t)$ and $(S^\tau, E^\tau, I^\tau, R^\tau) = (S, E, I, R)(t - \tau)$. To incorporate the effects of previous epidemiological states on avian influenza transmission and disease progression, we consider an SEIR epidemic model for birds with multiple distributed-time delays. The proposed delayed model is described by the following system of nonlinear integro-differential equations:

$$\begin{cases} \dot{S} &= \Lambda - \psi(I)S - \mu_s S, \\ \dot{E} &= \displaystyle\int_0^{\omega_1} \zeta_1(\tau) e^{-n_1\tau} \psi(I^\tau) S^\tau d\tau - \varepsilon E - \mu_e E, \\ \dot{I} &= \varepsilon \displaystyle\int_0^{\omega_2} \zeta_2(\tau) e^{-n_2\tau} E^\tau d\tau - \gamma I - \mu_i I, \\ \dot{R} &= \gamma \displaystyle\int_0^{\omega_3} \zeta_3(\tau) e^{-n_3\tau} I^\tau d\tau - \mu_r R. \end{cases} \tag{2.1}$$

Throughout this study, the incidence function ψ is assumed to be bounded, non-negative, increasing, and concave on $\mathbb{R}_+$. In addition, we assume that $\psi \in C^1(\mathbb{R}_+)$ and satisfies $\psi(0) = 0$. τ is treated as a random variable governed by the probability density functions $\zeta_i(\tau)$ over the intervals $[0, \omega_i]$, for $i = 1, 2, 3$. The quantity $\omega_i > 0$ represents the maximum possible duration of the corresponding delay. We assume that each function ζ_i is non-negative and normalized, namely,

$$\zeta_i(\tau) \geq 0, \qquad \tau \in [0, \omega_i],$$

and

$$\int_0^{\omega_i} \zeta_i(\tau)\, d\tau = 1.$$

Furthermore, the mean delay associated with each function is assumed to be finite; that is,

$$\int_0^{\omega_i} \tau\zeta_i(\tau)\, d\tau < \infty, \qquad i = 1, 2, 3.$$

To describe the biological meaning of the distributed-delay kernels, we make the following assumptions. The quantity $\zeta_1(\tau)e^{-n_1\tau}$ represents the probability density that a susceptible bird effectively exposed to avian influenza at time $t-\tau$ survives the delay period τ and enters the exposed class at time t. Thus, τ describes the time between effective infectious contact and the formation of the exposed class, while $1/n_1$ denotes the average survival time during this period. Similarly, $\zeta_2(\tau)e^{-n_2\tau}$ denotes the probability density that an exposed bird survives the latent period of length τ and becomes infectious at time t, where $1/n_2$ is the corresponding average survival time. Finally, $\zeta_3(\tau)e^{-n_3\tau}$ represents the probability density that an infectious bird survives for τ time units and then moves to the recovered class at time t, with $1/n_3$ denoting the average survival time during the recovery period.

Let us define the constants

$$F_i = \int_0^{\omega_i} \Pi_i(\tau)\, d\tau = \int_0^{\omega_i} \zeta_i(\tau)e^{-n_i\tau}\, d\tau, \qquad i = 1, 2, 3.$$

Here, F_i is the survival-weighted probability of completing the corresponding delayed transition.

In particular, $0 < F_i \leq 1$, because ζ_i is a probability density and $0 < e^{-n_i\tau} \leq 1$.

For the delayed avian influenza model (2.1), the initial conditions of the bird population are specified on the interval $[-\tau^*, 0]$ as follows:

$$\begin{cases} S(\theta) = \phi_1(\theta), \quad E(\theta) = \phi_2(\theta), \quad I(\theta) = \phi_3(\theta), \quad R(\theta) = \phi_4(\theta), \\ \phi_i(\theta) \geq 0, \quad i = 1, 2, 3, 4, \quad \theta \in [-\tau^*, 0]. \end{cases} \tag{2.2}$$

Here, $\tau^* = \max\{\omega_1, \omega_2, \omega_3\}$ represents the largest delay appearing in the model. The functions ϕ_i, $i = 1, 2, 3, 4$, describe the initial conditions of susceptible, exposed, infectious, and recovered birds, respectively. We assume that

$$\phi_i \in C([-\tau^*, 0], \mathbb{R}_{\geq 0}), \qquad i = 1, 2, 3, 4,$$

where $C([-\tau^*, 0], \mathbb{R}_{\geq 0})$ is the Banach space of continuous non-negative functions defined on $[-\tau^*, 0]$. This space is endowed with the supremum norm

$$\|\phi_i\| = \sup_{-\tau^* \leq \theta \leq 0} |\phi_i(\theta)|, \qquad i = 1, 2, 3, 4.$$

The quantities τ_i, $i = 1, 2, 3$, denote the delay parameters associated with the epidemiological transitions in the bird population. Moreover, n_i, $i = 1, 2, 3$, represent the mortality or removal rates during the corresponding delay periods, so that $1/n_i$ denotes the average survival time of birds in the ith delayed stage. The model variables and parameters are presented in Table 1.

Table 1. State variables and parameters of the avian influenza model.

Notation	Description	Units
$S(t)$	Number of susceptible birds at time t	Individuals
$E(t)$	Number of exposed birds at time t	Individuals
$I(t)$	Number of infectious birds at time t	Individuals
$R(t)$	Number of recovered birds at time t	Individuals
Λ	Recruitment rate of susceptible birds	Individuals/time
ψ	Saturated incidence function	1/time
ε	Progression rate from exposed to infectious	1/time
γ	Recovery rate of infectious birds	1/time
μ_s	Mortality rate of susceptible birds	1/time
μ_e	Mortality rate of exposed birds	1/time
μ_i	Mortality or removal rate of infectious birds	1/time
μ_r	Mortality rate of recovered birds	1/time
$\tau_i,\ i = 1, 2, 3$	Delay parameters	Time
$n_i,\ i = 1, 2, 3$	Mortality rates during delay periods	1/time
$\omega_i,\ i = 1, 2, 3$	Maximum admissible duration of distributed delay	Time

We first examine the reduced form of the proposed avian influenza model in the absence of distributed delays. The schematic representation of the proposed model is illustrated in Figure 1. This simplified system serves as a baseline model and provides the threshold quantities and stability results needed for comparison with the delayed formulation introduced later.

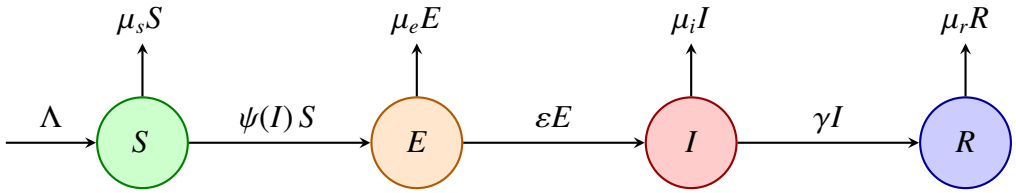


Figure 1. Flow diagram of the avian influenza transmission model in a bird population.

3. The non-delayed avian influenza model

In this section, we consider the avian influenza transmission model without distributed delays. In this case, the movements of birds between the susceptible, exposed, infectious, and recovered classes occur instantaneously according to the corresponding transition rates. The resulting generalized SEIR model is described by the following system of ordinary differential equations:

$$\begin{cases} \dot{S} &= \Lambda - \psi(I)S - \mu_s S, \\ \dot{E} &= \psi(I)S - (\varepsilon + \mu_e)E, \\ \dot{I} &= \varepsilon E - (\gamma + \mu_i)I, \\ \dot{R} &= \gamma I - \mu_r R. \end{cases} \tag{3.1}$$

Here, $S(t)$, $E(t)$, $I(t)$, and $R(t)$ denote the numbers of susceptible, exposed, infectious, and recovered birds at time t, respectively. The model is supplemented with the positive initial condition

$$(S(0), E(0), I(0), R(0)) = (S_0, E_0, I_0, R_0) \in \mathbb{R}^4_+.$$

3.1. Mathematical analysis

We begin by establishing some useful properties of the saturated incidence function ψ, which will be used in the subsequent analysis of the avian influenza model.

Lemma 1. *Assume that the incidence function ψ is non-negative, increasing, and concave and satisfies $\psi(0) = 0$. Then, for all $I > 0$, the following inequalities hold:*

$$\psi'(I)I \leq \psi(I) \leq \psi'(0)I.$$

Moreover, for all $I, I_1 > 0$, one has

$$\left(\frac{I}{I_1} - \frac{\psi(I)}{\psi(I_1)}\right)\left(\frac{\psi(I_1)}{\psi(I)} - 1\right) \leq 0.$$

Proof. Let $g_1(I) = \psi(I) - I\psi'(I)$. Since ψ is concave, we have $\psi''(I) \leq 0$. Hence,

$$g_1'(I) = -I\psi''(I) \geq 0.$$

Thus, g_1 is non-decreasing and $g_1(I) \geq g_1(0) = 0$. Therefore, $\psi(I) \geq I\psi'(I)$.

Next, define

$$g_2(I) = \psi(I) - I\psi'(0).$$

Since ψ is concave, $\psi'(I) \leq \psi'(0)$ for all $I > 0$. Consequently, $g_2'(I) = \psi'(I) - \psi'(0) \leq 0$. It follows that $g_2(I) \leq g_2(0) = 0$, which implies

$$\psi(I) \leq I\psi'(0).$$

To prove the second assertion, let

$$g_3(I) = \frac{\psi(I)}{I}, \qquad I > 0.$$

Then

$$g_3'(I) = \frac{I\psi'(I) - \psi(I)}{I^2} \leq 0,$$

by the first part of the lemma. Hence, g_3 is non-increasing. Since ψ is increasing, it follows that

$$(g_3(I) - g_3(I_1))\,(\psi(I) - \psi(I_1)) \leq 0.$$

That is,

$$\left(\frac{\psi(I)}{I} - \frac{\psi(I_1)}{I_1}\right)(\psi(I) - \psi(I_1)) \leq 0.$$

Equivalently,

$$\frac{\psi(I)\psi(I_1)}{I}\left(\frac{I}{I_1} - \frac{\psi(I)}{\psi(I_1)}\right)\left(\frac{\psi(I_1)}{\psi(I)} - 1\right) \leq 0.$$

Since $\psi(I) > 0$ and $\psi(I_1) > 0$ for $I, I_1 > 0$, we obtain

$$\left(\frac{I}{I_1} - \frac{\psi(I)}{\psi(I_1)}\right)\left(\frac{\psi(I_1)}{\psi(I)} - 1\right) \leq 0.$$

This completes the proof. □

Remark 1. *The assumption that ψ is concave plays two distinct roles in the critical-case analysis. First, it implies*

$$\psi(I) \leq \psi'(0)I,$$

which is essential for the Lyapunov estimates. Second, the nonlinear departure of $\psi(I)$ from its tangent at the origin, together with the negative feedback of infection on the susceptible population, determines the stabilizing quadratic term on the center manifold.

For the avian influenza model to be biologically meaningful, the state variables $S(t)$, $E(t)$, $I(t)$, and $R(t)$ must remain non-negative for all $t \geq 0$. We now show that the bird population is ultimately bounded in a positively invariant region. Let $\mu = \min\{\mu_s, \mu_e, \mu_i, \mu_r\}$.

Proposition 1. *The set*

$$\Omega_1 = \left\{(S, E, I, R) \in \mathbb{R}^4_+ : S + E + I + R \leq \frac{\Lambda}{\mu}\right\}$$

is a positively invariant compact region for model (3.1).

Proof. We first verify the non-negativity of solutions. On the boundary of the non-negative orthant, the right-hand sides of model (3.1) satisfy

$$\dot{S}\Big|_{S=0} = \Lambda > 0, \quad \dot{E}\Big|_{E=0} = \psi(I)S \geq 0, \quad \dot{I}\Big|_{I=0} = \varepsilon E \geq 0, \quad \text{and} \quad \dot{R}\Big|_{R=0} = \gamma I \geq 0.$$

Therefore, solutions that start in $\mathbb{R}^4_+$ remain non-negative for all $t \geq 0$.

Let

$$N(t) = S(t) + E(t) + I(t) + R(t)$$

denote the total bird population. By adding the equations of model (3.1), we obtain

$$\begin{aligned}\dot{N}(t) &= \dot{S} + \dot{E} + \dot{I} + \dot{R} \\ &= \Lambda - \mu_s S - \mu_e E - \mu_i I - \mu_r R \\ &\leq \Lambda - \mu(S + E + I + R) = \Lambda - \mu N(t).\end{aligned}$$

Thus,

$$\dot{N}(t) + \mu N(t) \leq \Lambda.$$

By the comparison theorem, it follows that

$$N(t) \leq N(0)e^{-\mu t} + \frac{\Lambda}{\mu}\left(1 - e^{-\mu t}\right).$$

In particular, if $N(0) \leq \Lambda/\mu$, then

$$N(t) \leq \frac{\Lambda}{\mu}, \qquad t \geq 0.$$

Hence, every solution that starts in Ω_1 remains in Ω_1 for all $t \geq 0$. Therefore, Ω_1 is a positively invariant compact region for the avian influenza model (3.1). □

To derive the basic reproduction number, we apply the next-generation matrix approach of Diekmann et al. and van den Driessche and Watmough [22,23]. We consider the infected compartments E and I and write the infected subsystem as

$$\begin{pmatrix} \dot{E} \\ \dot{I} \end{pmatrix} = \mathcal{F} - \mathcal{V}, \tag{3.2}$$

where

$$\mathcal{F} = \begin{pmatrix} \psi(I)S \\ 0 \end{pmatrix}, \quad \mathcal{V} = \begin{pmatrix} (\mu_e + \epsilon)E \\ -\epsilon E + (\mu_i + \gamma)I \end{pmatrix}. \tag{3.3}$$

At the disease-free equilibrium $DFE = (\Lambda/\mu_s, 0, 0, 0)$, the Jacobian matrices of $\mathcal{F}$ and $\mathcal{V}$ with respect to (E, I) are

$$F = \begin{pmatrix} 0 & \psi'(0)\Lambda/\mu_s \\ 0 & 0 \end{pmatrix}, \quad V = \begin{pmatrix} \mu_e + \epsilon & 0 \\ -\epsilon & \mu_i + \gamma \end{pmatrix}. \tag{3.4}$$

The next-generation matrix is FV^{-1}, and the basic reproduction number is the spectral radius of FV^{-1}:

$$\mathcal{R}_0 = \rho(FV^{-1}) = \frac{\Lambda\epsilon\psi'(0)}{\mu_s(\mu_e + \epsilon)(\mu_i + \gamma)}. \tag{3.5}$$

Epidemiologically, $\mathcal{R}_0$ represents the average number of secondary infections generated by a single infectious bird introduced into a completely susceptible bird population. The numerator $\Lambda\epsilon\psi'(0)$ captures the rate at which new infections are produced, while the denominator represents the losses from the exposed and infectious classes.

Proposition 2. *The avian influenza model* (3.1) *always admits a unique disease-free equilibrium*

$$DFE = \left(\frac{\Lambda}{\mu_s}, 0, 0, 0\right).$$

Moreover, if $\mathcal{R}_0 > 1$*, then model* (3.1) *admits a unique endemic equilibrium*

$$EE = (S^*, E^*, I^*, R^*),$$

where $S^* > 0,\ E^* > 0,\ I^* > 0,$ *and* $R^* > 0$.

Proof. At equilibrium, the right-hand side of model (3.1) satisfies

$$\begin{cases} 0 = \Lambda - \psi(I)S - \mu_s S, \\ 0 = \psi(I)S - (\mu_e + \varepsilon)E, \\ 0 = \varepsilon E - (\mu_i + \gamma)I, \\ 0 = \gamma I - \mu_r R. \end{cases} \tag{3.6}$$

From (3.6), we obtain

$$\begin{cases} S = \dfrac{\Lambda}{\mu_s + \psi(I)}, \\ E = \dfrac{\Lambda\psi(I)}{(\mu_e + \varepsilon)(\mu_s + \psi(I))}, \\ I = \dfrac{\varepsilon\Lambda\psi(I)}{(\mu_i + \gamma)(\mu_e + \varepsilon)(\mu_s + \psi(I))}, \\ R = \dfrac{\gamma}{\mu_r} I. \end{cases} \tag{3.7}$$

If $I = 0$, then $\psi(0) = 0$, and (3.6) gives $S = \frac{\Lambda}{\mu_s}$, $E = 0$, and $R = 0$. Thus, the disease-free equilibrium is uniquely given by

$$DFE = \left(\frac{\Lambda}{\mu_s}, 0, 0, 0\right).$$

We now consider the case $I > 0$. From (3.7), the infectious component must satisfy

$$I(\mu_i + \gamma)(\mu_e + \varepsilon)(\mu_s + \psi(I)) = \varepsilon\Lambda\psi(I).$$

Equivalently,

$$I\,G(I) = 0,$$

where

$$G(I) = (\mu_i + \gamma)(\mu_e + \varepsilon)(\mu_s + \psi(I)) - \varepsilon\Lambda\frac{\psi(I)}{I}, \qquad I > 0.$$

Differentiating G gives

$$G'(I) = (\mu_i + \gamma)(\mu_e + \varepsilon)\psi'(I) - \varepsilon\Lambda\frac{I\psi'(I) - \psi(I)}{I^2}.$$

By Lemma 1, we have

$$I\psi'(I) \le \psi(I),$$

and hence

$$\frac{I\psi'(I) - \psi(I)}{I^2} \le 0.$$

Therefore,

$$G'(I) \ge 0,$$

which shows that G is non-decreasing on $(0, \infty)$. In particular, under the standing assumptions on ψ, the equation $G(I) = 0$ can have at most one positive solution.

Using the definition of $\mathcal{R}_0$ in (3.5), we compute

$$\begin{aligned}\lim_{I\to 0^+} G(I) &= (\mu_i + \gamma)(\mu_e + \varepsilon)\mu_s - \varepsilon\Lambda\psi'(0)\\ &= \mu_s(\mu_i + \gamma)(\mu_e + \varepsilon)\left(1 - \mathcal{R}_0\right).\end{aligned}$$

Thus, if $\mathcal{R}_0 > 1$, then

$$\lim_{I\to 0^+} G(I) < 0.$$

On the other hand, since solutions are confined to the positively invariant region Ω_1, we have $0 < I \le \Lambda/\mu$, where

$$\mu = \min\{\mu_s, \mu_e, \mu_i, \mu_r\}.$$

Moreover,

$$\begin{aligned}G\left(\frac{\Lambda}{\mu}\right) &= (\mu_i + \gamma)(\mu_e + \varepsilon)\left(\mu_s + \psi\left(\frac{\Lambda}{\mu}\right)\right) - \mu\varepsilon\psi\left(\frac{\Lambda}{\mu}\right)\\ &= \mu_s(\mu_i + \gamma)(\mu_e + \varepsilon) + \psi\left(\frac{\Lambda}{\mu}\right)\left[(\mu_i + \gamma)(\mu_e + \varepsilon) - \mu\varepsilon\right].\end{aligned}$$

Since $\mu \leq \mu_i$, it follows that

$$(\mu_i + \gamma)(\mu_e + \varepsilon) - \mu\varepsilon > 0.$$

Consequently,

$$G\left(\frac{\Lambda}{\mu}\right) > 0.$$

Hence, when $\mathcal{R}_0 > 1$, the intermediate value theorem implies that there exists a positive solution $I^* \in (0, \Lambda/\mu)$ such that

$$G(I^*) = 0.$$

The monotonicity of G ensures that this positive solution is unique.

Therefore, model (3.1) has a unique endemic equilibrium

$$EE = (S^*, E^*, I^*, R^*)$$

when $\mathcal{R}_0 > 1$, where $S^* = \frac{\Lambda}{\mu_s + \psi(I^*)}$, $E^* = \frac{\Lambda\psi(I^*)}{(\mu_e+\varepsilon)(\mu_s+\psi(I^*))}$, and $R^* = \frac{\gamma}{\mu_r} I^*$. This completes the proof. □

3.2. Local stability analysis

In this subsection, we investigate the local stability of the equilibria of the non-delayed avian influenza model (3.1). The analysis is carried out in terms of the basic reproduction number $\mathcal{R}_0$.

Theorem 1. *The disease-free equilibrium*

$$DFE = \left(\frac{\Lambda}{\mu_s}, 0, 0, 0\right)$$

is locally asymptotically stable if $\mathcal{R}_0 < 1$ *and unstable if* $\mathcal{R}_0 > 1$.

Proof. Let (S, E, I, R) be a solution of model (3.1). The Jacobian matrix of the system is

$$J(S, E, I, R) = \begin{pmatrix} -(\mu_s + \psi(I)) & 0 & -\psi'(I)S & 0 \\ \psi(I) & -(\mu_e + \varepsilon) & \psi'(I)S & 0 \\ 0 & \varepsilon & -(\mu_i + \gamma) & 0 \\ 0 & 0 & \gamma & -\mu_r \end{pmatrix}.$$

Evaluating this matrix at the disease-free equilibrium gives

$$J(DFE) = \begin{pmatrix} -\mu_s & 0 & -\psi'(0)\dfrac{\Lambda}{\mu_s} & 0 \\ 0 & -(\mu_e + \varepsilon) & \psi'(0)\dfrac{\Lambda}{\mu_s} & 0 \\ 0 & \varepsilon & -(\mu_i + \gamma) & 0 \\ 0 & 0 & \gamma & -\mu_r \end{pmatrix}.$$

Two eigenvalues are immediately obtained as

$$\lambda_1 = -\mu_s < 0, \qquad \lambda_2 = -\mu_r < 0.$$

The remaining two eigenvalues are determined by the submatrix

$$M = \begin{pmatrix} -(\mu_e + \varepsilon) & \psi'(0)\dfrac{\Lambda}{\mu_s} \\ \varepsilon & -(\mu_i + \gamma) \end{pmatrix}.$$

The trace and determinant of M are given by

$$\mathrm{tr}(M) = -(\mu_e + \varepsilon + \mu_i + \gamma) < 0,$$

and

$$\begin{aligned} \det(M) &= (\mu_e + \varepsilon)(\mu_i + \gamma) - \varepsilon\psi'(0)\frac{\Lambda}{\mu_s} \\ &= (\mu_e + \varepsilon)(\mu_i + \gamma)(1 - \mathcal{R}_0). \end{aligned}$$

If $\mathcal{R}_0 < 1$, then $\det(M) > 0$ and $\mathrm{tr}(M) < 0$; hence, the two eigenvalues of M have negative real parts. Therefore, all eigenvalues of $J(DFE)$ have negative real parts, and the disease-free equilibrium is locally asymptotically stable.

If $\mathcal{R}_0 > 1$, then $\det(M) < 0$, which implies that M has one positive eigenvalue. Consequently, the disease-free equilibrium is unstable. □

Theorem 2. *Assume that* $\mathcal{R}_0 > 1$. *Then the endemic equilibrium*

$$EE = (S^*, E^*, I^*, R^*)$$

of model (3.1) *is locally asymptotically stable.*

Proof. At the endemic equilibrium, the Jacobian matrix becomes

$$J(EE) = \begin{pmatrix} -(\mu_s + \psi(I^*)) & 0 & -\psi'(I^*)S^* & 0 \\ \psi(I^*) & -(\mu_e + \varepsilon) & \psi'(I^*)S^* & 0 \\ 0 & \varepsilon & -(\mu_i + \gamma) & 0 \\ 0 & 0 & \gamma & -\mu_r \end{pmatrix}.$$

For simplicity, define

$$A = \mu_s + \psi(I^*), \qquad B = \mu_e + \varepsilon, \qquad C = \mu_i + \gamma, \qquad q = \psi'(I^*)S^*.$$

Since $\lambda = -\mu_r$ is one eigenvalue, the remaining eigenvalues are the roots of the cubic polynomial

$$Q(\lambda) = (\lambda + A)\left[(\lambda + B)(\lambda + C) - \varepsilon q\right] + \varepsilon\psi(I^*)q.$$

Equivalently,

$$Q(\lambda) = \lambda^3 + a_2\lambda^2 + a_1\lambda + a_0,$$

where

$$\begin{aligned} a_2 &= A + B + C, \\ a_1 &= A(B + C) + BC - \varepsilon q, \end{aligned}$$

and

$$a_0 = A(BC - \varepsilon q) + \varepsilon\psi(I^*)q.$$

From the equilibrium relations, we have $\varepsilon E^* = (\mu_i + \gamma)I^*$ and $E^* = \frac{\psi(I^*)S^*}{\mu_e+\varepsilon}$. Therefore,

$$\varepsilon\frac{\psi(I^*)S^*}{I^*} = (\mu_e + \varepsilon)(\mu_i + \gamma) = BC.$$

Moreover, by Lemma 1,

$$\psi'(I^*) \leq \frac{\psi(I^*)}{I^*}.$$

It follows that

$$\varepsilon q = \varepsilon\psi'(I^*)S^* \leq \varepsilon\frac{\psi(I^*)S^*}{I^*} = BC.$$

Hence,

$$BC - \varepsilon q \geq 0.$$

Using this inequality, we obtain

$$a_2 = A + B + C > 0,$$

$$a_1 = A(B + C) + BC - \varepsilon q > 0,$$

and

$$a_0 = A(BC - \varepsilon q) + \varepsilon\psi(I^*)q > 0.$$

It remains to verify the Routh–Hurwitz condition

$$a_2a_1 - a_0 > 0.$$

Indeed,

$$\begin{aligned} a_2a_1 - a_0 &= (A + B + C)[A(B + C) + BC - \varepsilon q] \\ &\quad - [A(BC - \varepsilon q) + \varepsilon\psi(I^*)q] \\ &= A(A + B + C)(B + C) + (B + C)(BC - \varepsilon q) - \varepsilon\psi(I^*)q. \end{aligned}$$

Since $BC - \varepsilon q \geq 0$ and $A = \mu_s + \psi(I^*) > \psi(I^*)$, we have

$$A(A + B + C)(B + C) > \psi(I^*)BC.$$

Furthermore, $\varepsilon q \leq BC$, and therefore

$$\varepsilon\psi(I^*)q \leq \psi(I^*)BC.$$

Consequently,

$$a_2a_1 - a_0 > 0.$$

Thus,

$$a_2 > 0, \qquad a_1 > 0, \qquad a_0 > 0, \qquad a_2a_1 > a_0.$$

By the Routh–Hurwitz criterion, all roots of $Q(\lambda)$ have negative real parts. Since the remaining eigenvalue is $\lambda = -\mu_r < 0$, all eigenvalues of $J(EE)$ have negative real parts. Therefore, the endemic equilibrium is locally asymptotically stable whenever $\mathcal{R}_0 > 1$. □

3.3. Global stability analysis

In this subsection, we study the global dynamics of the non-delayed avian influenza model (3.1). The purpose is to determine whether solutions approach the disease-free equilibrium or the endemic equilibrium, depending on the threshold value $\mathcal{R}_0$.

Lemma 2. *The set*

$$\Omega_2 = \left\{(S, E, I, R) \in \mathbb{R}^4_+ : S + E + I + R \leq \frac{\Lambda}{\mu},\ S \leq \frac{\Lambda}{\mu_s}\right\}$$

is a positively invariant region for model (3.1).

Proof. From Proposition 1, the set

$$\Omega_1 = \left\{(S, E, I, R) \in \mathbb{R}^4_+ : S + E + I + R \leq \frac{\Lambda}{\mu}\right\}$$

is positively invariant. It remains to verify the upper bound for the susceptible bird population. From the first equation of model (3.1), we have

$$\dot{S} = \Lambda - \mu_s S - \psi(I)S \leq \Lambda - \mu_s S.$$

On the boundary $S = \Lambda/\mu_s$, it follows that

$$\dot{S} \leq \Lambda - \mu_s\left(\frac{\Lambda}{\mu_s}\right) = 0.$$

Thus, the vector field points inward on the boundary $S = \Lambda/\mu_s$. Hence, any solution that starts with $S(0) \leq \Lambda/\mu_s$ satisfies

$$S(t) \leq \frac{\Lambda}{\mu_s}, \qquad t \geq 0.$$

Therefore, Ω_2 is positively invariant for the avian influenza model (3.1). □

Theorem 3. *The disease-free equilibrium*

$$E_0 = \left(\frac{\Lambda}{\mu_s}, 0, 0, 0\right)$$

of system (3.1) *is globally asymptotically stable in* Ω_2 *when* $\mathcal{R}_0 \leq 1$.

Proof. Let $\bar{S}_0 = \dfrac{\Lambda}{\mu_s}$ and define the candidate Lyapunov function $\mathcal{L}_1(S, E, I, R)$ as follows:

$$\mathcal{L}_1 = S - \bar{S}_0 - \bar{S}_0 \ln\left(\frac{S}{\bar{S}_0}\right) + E + \frac{(\mu_e + \varepsilon)}{\varepsilon} I.$$

Calculating $\dfrac{d\mathcal{L}_1}{dt}$ along the solution of system (3.1) gives

$$\frac{d\mathcal{L}_1}{dt} = \left(1 - \frac{\bar{S}_0}{S}\right)\dot{S} + \dot{E} + \frac{(\mu_e + \varepsilon)}{\varepsilon}\dot{I}.$$

From system (3.1) we obtain

$$\begin{aligned}
\frac{d\mathcal{L}_1}{dt} &= \left(1-\frac{\bar{S}_0}{S}\right)(\Lambda-\psi(I)S-\mu_s S)+\psi(I)S-(\varepsilon+\mu_e)E+\frac{(\mu_e+\varepsilon)}{\varepsilon}(\varepsilon E-(\gamma+\mu_i)I)\\
&= \left(1-\frac{\bar{S}_0}{S}\right)(\Lambda-\mu_s S)-\psi(I)S+\psi(I)\bar{S}_0+\psi(I)S-(\varepsilon+\mu_e)E+(\mu_e+\varepsilon)E-\frac{(\mu_e+\varepsilon)(\mu_i+\gamma)}{\varepsilon}I\\
&= \left(1-\frac{\bar{S}_0}{S}\right)(\Lambda-\mu_s S)+\psi(I)\bar{S}_0-\frac{(\mu_i+\gamma)(\mu_e+\varepsilon)}{\varepsilon}I\\
&= -\frac{\mu_s}{S}\left(S-\bar{S}_0\right)^2+\psi(I)\bar{S}_0-\frac{(\mu_i+\gamma)(\mu_e+\varepsilon)}{\varepsilon}I\\
&\leq -\frac{\mu_s}{S}\left(S-\bar{S}_0\right)^2+\psi'(0)I\bar{S}_0-\frac{(\mu_i+\gamma)(\mu_e+\varepsilon)}{\varepsilon}I\\
&= -\frac{\mu_s}{S}\left(S-\bar{S}_0\right)^2+\frac{(\mu_i+\gamma)(\mu_e+\varepsilon)}{\varepsilon}\left(\frac{\varepsilon\psi'(0)\bar{S}_0}{(\mu_i+\gamma)(\mu_e+\varepsilon)}-1\right)I\\
&= -\frac{\mu_s}{S}\left(S-\bar{S}_0\right)^2+\frac{(\mu_i+\gamma)(\mu_e+\varepsilon)}{\varepsilon}(\mathcal{R}_0-1)\,I.
\end{aligned}$$

Therefore, for all $S, E, I, R > 0$ we have $\frac{d\mathcal{L}_1}{dt} \leq 0$ when $\mathcal{R}_0 \leq 1$. Moreover, $\frac{d\mathcal{L}_1}{dt} = 0$ when $S = \bar{S}_0$ and $(\mathcal{R}_0 - 1)I = 0$. According to [24], solutions of system (3.1) converge to the largest invariant subset of $\mathcal{M}_1 = \left\{(S, E, I, R) \in \Omega_2 : \dot{\mathcal{L}}_1 = 0\right\}$, which contains elements with $S(t) = \bar{S}_0$ and

$$(\mathcal{R}_0 - 1)I = 0. \tag{3.8}$$

Let us consider two cases:

- If $\mathcal{R}_0 < 1$, then from Eq (3.8), we obtain $I = 0$. Since Ω_0 is invariant, $\dot{I}(t) = 0$. From the third equation of system (3.1), we have

$$0 = \dot{I} = \varepsilon E \Rightarrow E(t) = 0, \text{ for any } t. \tag{3.9}$$

  Furthermore, since $I = 0$, $\lim_{t\to\infty} R(t) = 0$. Hence, $\mathcal{M}_1 = \{\mathcal{E}_0\}$.
- If $\mathcal{R}_0 = 1$, we have $S = \bar{S}_0$, and then $\dot{S}(t) = 0$. From the first equation of system (3.1), we have

$$\Lambda - \psi(I)S - \mu_s S = 0 \Longrightarrow \psi(I(t))\bar{S}_0 = 0, \text{ for any } t. \tag{3.10}$$

  This implies that $I(t) = 0$ for all $t \geq 0$. As in the first case, from the third equation of system (3.1), we get $E(t) = 0$, for any t. Furthermore, since $I = 0$, $\lim_{t\to\infty} R(t) = 0$. Hence, $\mathcal{M}_1 = \{\mathcal{E}_0\}$.

LaSalle's invariance principle [25] reveals that $\mathcal{E}_0 = \left(\bar{S}_0, 0, 0, 0\right)$ is globally asymptotically stable (GAS) only if $\mathcal{R}_0 \leq 1$. □

Theorem 4. *If $\mathcal{R}_0 > 1$, then the endemic equilibrium*

$$\mathcal{E}^* = (S^*, E^*, I^*, R^*)$$

of model (3.1) *is globally asymptotically stable in the interior of Ω_2.*

Proof. Assume that $\mathcal{R}_0 > 1$, so that the endemic equilibrium $\mathcal{E}^*$ exists and is unique. Define the Lyapunov function

$$\mathcal{L}_2(S, E, I) = \left(S - S^* \ln \frac{S}{S^*}\right) + \left(E - E^* \ln \frac{E}{E^*}\right) + \frac{\mu_e + \varepsilon}{\varepsilon}\left(I - I^* \ln \frac{I}{I^*}\right).$$

This function is well defined and non-negative up to an additive constant for all $S, E, I > 0$, and it attains its minimum at

$$S = S^*, \qquad E = E^*, \qquad I = I^*.$$

Differentiating $\mathcal{L}_2$ along the solutions of model (3.1) gives

$$\dot{\mathcal{L}}_2 = \left(1 - \frac{S^*}{S}\right)\dot{S} + \left(1 - \frac{E^*}{E}\right)\dot{E} + \frac{\mu_e + \varepsilon}{\varepsilon}\left(1 - \frac{I^*}{I}\right)\dot{I}.$$

Using model (3.1), we obtain

$$\begin{aligned}\dot{\mathcal{L}}_2 = &\left(1 - \frac{S^*}{S}\right)(\Lambda - \mu_s S - \psi(I)S) \\ &+ \left(1 - \frac{E^*}{E}\right)(\psi(I)S - (\mu_e + \varepsilon)E) \\ &+ \frac{\mu_e + \varepsilon}{\varepsilon}\left(1 - \frac{I^*}{I}\right)(\varepsilon E - (\mu_i + \gamma)I).\end{aligned}$$

At the endemic equilibrium, the following identities hold:

$$\Lambda = \mu_s S^* + \psi(I^*)S^*,$$

$$\psi(I^*)S^* = (\mu_e + \varepsilon)E^*,$$

and

$$\varepsilon E^* = (\mu_i + \gamma)I^*.$$

Substituting these relations into the expression for $\dot{\mathcal{L}}_2$ and simplifying yield

$$\begin{aligned}\dot{\mathcal{L}}_2 = &\mu_s\left(1 - \frac{S^*}{S}\right)(S^* - S) \\ &+ \psi(I^*)S^*\left[4 - \frac{S^*}{S} - \frac{E}{E^*}\frac{I^*}{I} - \frac{I}{I^*}\frac{\psi(I^*)}{\psi(I)} - \frac{S}{S^*}\frac{E^*}{E}\frac{\psi(I)}{\psi(I^*)}\right] \\ &+ \psi(I^*)S^*\left(\frac{I}{I^*} - \frac{\psi(I)}{\psi(I^*)}\right)\left(\frac{\psi(I^*)}{\psi(I)} - 1\right).\end{aligned}$$

The first term is non-positive, since

$$\mu_s\left(1 - \frac{S^*}{S}\right)(S^* - S) = -\mu_s\frac{(S - S^*)^2}{S} \leq 0.$$

For the second term, we apply the arithmetic–geometric mean inequality:

$$x_1 + x_2 + x_3 + x_4 \geq 4\sqrt[4]{x_1 x_2 x_3 x_4}, \qquad x_j \geq 0.$$

Taking

$$x_1 = \frac{S^*}{S}, \quad x_2 = \frac{E}{E^*}\frac{I^*}{I}, \quad x_3 = \frac{I}{I^*}\frac{\psi(I^*)}{\psi(I)}, \quad x_4 = \frac{S}{S^*}\frac{E^*}{E}\frac{\psi(I)}{\psi(I^*)},$$

we note that

$$x_1 x_2 x_3 x_4 = 1.$$

Hence,

$$4 - \frac{S^*}{S} - \frac{E}{E^*}\frac{I^*}{I} - \frac{I}{I^*}\frac{\psi(I^*)}{\psi(I)} - \frac{S}{S^*}\frac{E^*}{E}\frac{\psi(I)}{\psi(I^*)} \leq 0.$$

Finally, by Lemma 1, we have

$$\left(\frac{I}{I^*} - \frac{\psi(I)}{\psi(I^*)}\right)\left(\frac{\psi(I^*)}{\psi(I)} - 1\right) \leq 0.$$

Therefore,

$$\dot{\mathcal{L}}_2 \leq 0$$

for all positive solutions in Ω_2.

It remains to identify the largest invariant set contained in

$$\mathcal{M}_2 = \left\{(S, E, I, R) \in \Omega_2 : \dot{\mathcal{L}}_2 = 0\right\}.$$

The equality $\dot{\mathcal{L}}_2 = 0$ requires

$$S = S^*$$

and

$$\frac{E}{E^*} = \frac{I}{I^*}.$$

Let

$$\frac{E}{E^*} = \frac{I}{I^*} = a.$$

Then

$$E = aE^*, \qquad I = aI^*.$$

Substitution into the equilibrium relations and the model equations shows that the only invariant possibility is

$$a = 1.$$

Thus,

$$S = S^*, \qquad E = E^*, \qquad I = I^*.$$

Moreover, since

$$\dot{R} = \gamma I - \mu_r R,$$

and $I = I^*$ on the invariant set, the equation for R gives

$$R = \frac{\gamma}{\mu_r} I^* = R^*.$$

Hence, the largest invariant subset of $\mathcal{M}_2$ is the singleton

$$\{\mathcal{E}^*\}.$$

By LaSalle's invariance principle [26], the endemic equilibrium $\mathcal{E}^*$ is globally asymptotically stable in the interior of Ω_2 whenever $\mathcal{R}_0 > 1$. □

4. The distributed-delay avian influenza model

We now return to the full avian influenza model (2.1), in which distributed delays are incorporated to describe the time lags associated with the formation of exposed, infectious, and recovered bird classes. Before studying the threshold dynamics of the delayed system, we establish the non-negativity and ultimate boundedness of its solutions.

Lemma 3. *For any non-negative initial conditions satisfying* (2.2)*, the delayed avian influenza model* (2.1) *admits a unique non-negative solution. Moreover, all solutions are ultimately bounded. More precisely,*

$$\limsup_{t\to\infty} S(t) \le \Gamma_1,\ \limsup_{t\to\infty} E(t) \le \Gamma_2,\ \limsup_{t\to\infty} I(t) \le \Gamma_3,\ \limsup_{t\to\infty} R(t) \le \Gamma_4,$$

where $\Gamma_1 = \dfrac{\Lambda}{\mu_s}$, $\Gamma_2 = \dfrac{\Lambda F_1}{\sigma_1}$, $\Gamma_3 = \dfrac{\varepsilon F_2 \Gamma_2}{\gamma + \mu_i}$, $\Gamma_4 = \dfrac{\gamma F_3 \Gamma_3}{\mu_r}$, *and* $\sigma_1 = \min\{\mu_s, \varepsilon + \mu_e\}$. *Consequently, for every* $\delta > 0$*, there exists* $T_\delta > 0$ *such that*

$$S(t) \le \Gamma_1 + \delta,\ E(t) \le \Gamma_2 + \delta,\ I(t) \le \Gamma_3 + \delta,\ R(t) \le \Gamma_4 + \delta$$

for all $t \ge T_\delta$.

Proof. The existence and uniqueness of solutions follow from the standard theory of functional differential equations, since the right-hand side of (2.1) is continuous and locally Lipschitz with respect to the state variables under the assumptions imposed on ψ and the delay kernels.

We first prove non-negativity. From the first equation of (2.1), we have

$$\dot{S}\big|_{S=0} = \Lambda > 0.$$

Thus, the susceptible bird population cannot become negative. For the remaining state variables, the variation-of-constants formula gives

$$E(t) = e^{-(\varepsilon+\mu_e)t}\phi_2(0) + \int_0^t e^{-(\varepsilon+\mu_e)(t-\theta)} \int_0^{\omega_1} \Pi_1(\tau)\psi(I(\theta-\tau))S(\theta-\tau)\,d\tau\,d\theta \ge 0,$$

$$I(t) = e^{-(\gamma+\mu_i)t}\phi_3(0) + \varepsilon \int_0^t e^{-(\gamma+\mu_i)(t-\theta)} \int_0^{\omega_2} \Pi_2(\tau)E(\theta-\tau)\,d\tau\,d\theta \ge 0,$$

and

$$R(t) = e^{-\mu_r t}\phi_4(0) + \gamma \int_0^t e^{-\mu_r(t-\theta)} \int_0^{\omega_3} \Pi_3(\tau)I(\theta-\tau)\,d\tau\,d\theta \ge 0.$$

Since the initial functions are non-negative on $[-\tau^*, 0]$, it follows by a standard continuation argument that

$$S(t) \ge 0, \qquad E(t) \ge 0, \qquad I(t) \ge 0, \qquad R(t) \ge 0, \qquad t \ge 0.$$

We next establish ultimate boundedness. From the susceptible equation,

$$\dot{S}(t) = \Lambda - \psi(I(t))S(t) - \mu_s S(t) \le \Lambda - \mu_s S(t).$$

Hence, by comparison,

$$\limsup_{t\to\infty} S(t) \le \frac{\Lambda}{\mu_s} = \Gamma_1.$$

To obtain an upper bound for the exposed class, define

$$Y_1(t) = \int_0^{\omega_1} \Pi_1(\tau) S(t-\tau)\, d\tau + E(t).$$

Differentiating $Y_1(t)$ along solutions of (2.1), we obtain

$$\begin{aligned}
\dot{Y}_1(t) &= \int_0^{\omega_1} \Pi_1(\tau)\dot{S}(t-\tau)\, d\tau + \dot{E}(t) \\
&= \int_0^{\omega_1} \Pi_1(\tau)\left[\Lambda - \psi(I(t-\tau))S(t-\tau) - \mu_s S(t-\tau)\right] d\tau \\
&\quad + \int_0^{\omega_1} \Pi_1(\tau)\psi(I(t-\tau))S(t-\tau)\, d\tau - (\varepsilon+\mu_e)E(t) \\
&= \Lambda F_1 - \mu_s \int_0^{\omega_1} \Pi_1(\tau) S(t-\tau)\, d\tau - (\varepsilon+\mu_e)E(t).
\end{aligned}$$

Therefore,

$$\dot{Y}_1(t) \le \Lambda F_1 - \sigma_1 Y_1(t),$$

where

$$\sigma_1 = \min\{\mu_s, \varepsilon + \mu_e\}.$$

By the comparison theorem,

$$\limsup_{t\to\infty} Y_1(t) \le \frac{\Lambda F_1}{\sigma_1}.$$

Since $E(t) \le Y_1(t)$, we have

$$\limsup_{t\to\infty} E(t) \le \Gamma_2, \qquad \Gamma_2 = \frac{\Lambda F_1}{\sigma_1}.$$

For the infectious bird class, the third equation of (2.1) yields

$$\begin{aligned}
\dot{I}(t) &= \varepsilon \int_0^{\omega_2} \Pi_2(\tau) E(t-\tau)\, d\tau - (\gamma+\mu_i) I(t) \\
&\le \varepsilon F_2 \Gamma_2 - (\gamma+\mu_i) I(t).
\end{aligned}$$

Thus,

$$\limsup_{t\to\infty} I(t) \le \Gamma_3, \qquad \Gamma_3 = \frac{\varepsilon F_2 \Gamma_2}{\gamma+\mu_i}.$$

Finally, the recovered bird class satisfies

$$\begin{aligned}
\dot{R}(t) &= \gamma \int_0^{\omega_3} \Pi_3(\tau) I(t-\tau)\, d\tau - \mu_r R(t) \\
&\le \gamma F_3 \Gamma_3 - \mu_r R(t).
\end{aligned}$$

Hence,

$$\limsup_{t\to\infty} R(t) \le \Gamma_4, \qquad \Gamma_4 = \frac{\gamma F_3 \Gamma_3}{\mu_r}.$$

Consequently, all solutions of the delayed avian influenza model are non-negative and ultimately bounded. □

Based on Lemma 3, one can show that the bounded region

$$\Omega^d = \left\{(S, E, I, R) \in \mathbb{R}^4_+ : 0 \le S \le \Gamma_1,\ 0 \le E \le \Gamma_2,\ 0 \le I \le \Gamma_3,\ 0 \le R \le \Gamma_4\right\}$$

is positively invariant w.r.t. system (2.1).

We now derive the corresponding basic reproduction number and characterize the equilibrium points of the distributed-delay model.

For the delayed model, the next-generation approach [22, 23] must account for the survival factors introduced by the delays. The infected subsystem is

$$\begin{pmatrix} \dot{E} \\ \dot{I} \end{pmatrix} = \mathcal{F}_d - \mathcal{V}_d, \tag{4.1}$$

where

$$\mathcal{F}_d = \begin{pmatrix} \int_0^{\omega_1} \zeta_1(\tau) e^{-n_1\tau} \psi(I^\tau) S^\tau d\tau \\ 0 \end{pmatrix}, \quad \mathcal{V}_d = \begin{pmatrix} (\mu_e + \epsilon)E \\ -\varepsilon \int_0^{\omega_2} \zeta_2(\tau) e^{-n_2\tau} E^\tau d\tau + (\mu_i + \gamma)I \end{pmatrix}. \tag{4.2}$$

At the disease-free equilibrium, $\mathcal{E}_0$, the Jacobian matrices are

$$F_d = \begin{pmatrix} 0 & F_1\psi'(0)\Lambda/\mu_s \\ 0 & 0 \end{pmatrix}, \qquad V_d = \begin{pmatrix} \mu_e + \epsilon & 0 \\ -\epsilon F_2 & \mu_i + \gamma \end{pmatrix}. \tag{4.3}$$

The delayed basic reproduction number is therefore

$$\mathcal{R}_d = \rho(F_d V_d^{-1}) = \frac{\epsilon \Lambda F_1 F_2 \psi'(0)}{\mu_s(\mu_e + \epsilon)(\mu_i + \gamma)}. \tag{4.4}$$

The survival factors F_1 and F_2 represent the probabilities that birds survive the latency and transition periods, respectively, and their inclusion reduces the effective transmission potential compared to the non-delayed case.

Lemma 4. *The distributed-delay avian influenza model* (2.1) *admits the disease-free equilibrium*

$$\mathcal{E}_0 = \left(\frac{\Lambda}{\mu_s}, 0, 0, 0\right).$$

If $\mathcal{R}_d > 1$*, then model* (2.1) *has a unique endemic equilibrium*

$$\mathcal{E}^* = (S^*, E^*, I^*, R^*),$$

where all components are positive.

Proof. At equilibrium, the state variables are constant. Therefore, the distributed delay terms reduce to the survival-weighted factors F_i, $i = 1, 2, 3$. Setting the right-hand side of (2.1) equal to zero gives

$$\begin{cases} 0 = \Lambda - \psi(I)S - \mu_s S, \\ 0 = F_1\psi(I)S - (\mu_e + \varepsilon)E, \\ 0 = \varepsilon F_2 E - (\mu_i + \gamma)I, \\ 0 = \gamma F_3 I - \mu_r R. \end{cases} \tag{4.5}$$

From (4.5), we obtain

$$\begin{cases} S = \dfrac{\Lambda}{\mu_s + \psi(I)}, \\ E = \dfrac{\Lambda F_1 \psi(I)}{(\mu_e + \varepsilon)(\mu_s + \psi(I))}, \\ I = \dfrac{\varepsilon\Lambda F_1 F_2 \psi(I)}{(\mu_i + \gamma)(\mu_e + \varepsilon)(\mu_s + \psi(I))}, \\ R = \dfrac{\gamma F_3}{\mu_r} I. \end{cases} \tag{4.6}$$

If $I = 0$, then $\psi(0) = 0$, and (4.5) gives

$$S = \frac{\Lambda}{\mu_s}, \qquad E = 0, \qquad R = 0.$$

Hence, the disease-free equilibrium is

$$\mathcal{E}_0 = \left(\frac{\Lambda}{\mu_s}, 0, 0, 0\right).$$

We now consider the existence of a positive endemic equilibrium. For $I > 0$, (4.6) implies

$$I(\mu_i + \gamma)(\mu_e + \varepsilon)(\mu_s + \psi(I)) = \varepsilon\Lambda F_1 F_2 \psi(I).$$

Equivalently,

$$I\,G(I) = 0,$$

where

$$G(I) = (\mu_i + \gamma)(\mu_e + \varepsilon)(\mu_s + \psi(I)) - \varepsilon\Lambda F_1 F_2 \frac{\psi(I)}{I}, \qquad I > 0.$$

Differentiating G gives

$$G'(I) = (\mu_i + \gamma)(\mu_e + \varepsilon)\psi'(I) - \varepsilon\Lambda F_1 F_2 \frac{I\psi'(I) - \psi(I)}{I^2}.$$

By Lemma 1,

$$I\psi'(I) \le \psi(I),$$

and hence

$$G'(I) \ge 0.$$

Thus, G is non-decreasing on $(0, \infty)$.

Furthermore,

$$\lim_{I\to 0^+} G(I) = \mu_s(\mu_i+\gamma)(\mu_e+\varepsilon) - \varepsilon\Lambda F_1F_2\psi'(0)$$
$$= \mu_s(\mu_i+\gamma)(\mu_e+\varepsilon)\left(1-\mathcal{R}_d\right).$$

Therefore, if $\mathcal{R}_d > 1$, then

$$\lim_{I\to 0^+} G(I) < 0.$$

On the other hand, since $0 < F_1F_2 \leq 1$ and

$$\mu = \min\{\mu_s, \mu_e, \mu_i, \mu_r\},$$

we have

$$G\left(\frac{\Lambda}{\mu}\right) = (\mu_i+\gamma)(\mu_e+\varepsilon)\left(\mu_s+\psi\left(\frac{\Lambda}{\mu}\right)\right) - \mu\varepsilon F_1F_2\psi\left(\frac{\Lambda}{\mu}\right)$$
$$= \mu_s(\mu_i+\gamma)(\mu_e+\varepsilon) + \psi\left(\frac{\Lambda}{\mu}\right)\left[(\mu_i+\gamma)(\mu_e+\varepsilon) - \mu\varepsilon F_1F_2\right].$$

Since

$$(\mu_i+\gamma)(\mu_e+\varepsilon) - \mu\varepsilon F_1F_2 > 0,$$

it follows that

$$G\left(\frac{\Lambda}{\mu}\right) > 0.$$

Thus, when $\mathcal{R}_d > 1$, the intermediate value theorem implies that there exists at least one positive solution

$$I^* \in \left(0, \frac{\Lambda}{\mu}\right)$$

such that

$$G(I^*) = 0.$$

Since G is non-decreasing, this positive solution is unique.

Consequently, the endemic equilibrium is uniquely determined by $S^* = \dfrac{\Lambda}{\mu_s+\psi(I^*)}$, $E^* = \dfrac{\Lambda F_1\psi(I^*)}{(\mu_e+\varepsilon)(\mu_s+\psi(I^*))}$, $I^* > 0$, and $R^* = \dfrac{\gamma F_3}{\mu_r}I^*$. Hence, the distributed-delay avian influenza model admits a unique endemic equilibrium whenever $\mathcal{R}_d > 1$. □

Global stability analysis

In this subsection, we examine the global dynamics of the distributed-delay avian influenza model (2.1). The aim is to determine the long-term behavior of the bird population in relation to the delayed basic reproduction number $\mathcal{R}_d$.

Theorem 5. *If $\mathcal{R}_d \leq 1$, then the disease-free equilibrium*

$$\mathcal{E}_0^d = \left(\frac{\Lambda}{\mu_s}, 0, 0, 0\right)$$

is globally asymptotically stable in the feasible region of model (2.1).

Proof. Let $\bar{S}_0 = \dfrac{\Lambda}{\mu_s}$ and define the candidate Lyapunov function $\mathcal{L}_1^d(S, E, I, R)$ as follows:

$$\mathcal{L}_1^d = F_1F_2\left(S - \bar{S}_0 - \bar{S}_0 \ln\left(\frac{S}{\bar{S}_0}\right)\right) + F_2E + \frac{(\mu_e+\varepsilon)}{\varepsilon}I$$
$$+ F_2\int_0^{\omega_1}\Pi_1(\tau)\int_{t-\tau}^{t}\psi(I(\theta))S(\theta)\,d\theta\,d\tau + (\mu_e+\varepsilon)\int_0^{\omega_2}\Pi_2(\tau)\int_{t-\tau}^{t}E(\theta)\,d\theta\,d\tau.$$

Calculating $\dfrac{d\mathcal{L}_1^d}{dt}$ along the solution of system (2.1) gives

$$\begin{aligned}
\frac{d\mathcal{L}_1^d}{dt} &= F_1F_2\left(1-\frac{\bar{S}_0}{S}\right)(\Lambda - \psi(I)S - \mu_sS) + F_2\left(\int_0^{\omega_1}\Pi_1(\tau)\psi(I^\tau)S^\tau d\tau - (\varepsilon+\mu_e)E\right)\\
&+ \frac{(\mu_e+\varepsilon)}{\varepsilon}\left(\varepsilon\int_0^{\omega_2}\Pi_2(\tau)E^\tau d\tau - (\gamma+\mu_i)I\right)\\
&+ F_2\int_0^{\omega_1}\Pi_1(\tau)(\psi(I)S - \psi(I^\tau)S^\tau)\,d\tau + (\mu_e+\varepsilon)\int_0^{\omega_2}\Pi_2(\tau)(E-E^\tau)\,d\tau\\
&= F_1F_2\left(1-\frac{\bar{S}_0}{S}\right)(\Lambda - \psi(I)S - \mu_sS) + F_2\,(F_1\psi(I)S - (\varepsilon+\mu_e)E)\\
&+ \frac{(\mu_e+\varepsilon)}{\varepsilon}\,(\varepsilon F_2E - (\gamma+\mu_i)I)\\
&= -F_1F_2\frac{\mu_s}{S}\left(S-\bar{S}_0\right)^2 + F_1F_2\psi(I)\bar{S}_0 - \frac{(\mu_e+\varepsilon)(\gamma+\mu_i)}{\varepsilon}I\\
&\le -F_1F_2\frac{\mu_s}{S}\left(S-\bar{S}_0\right)^2 + F_1F_2\psi'(0)I\bar{S}_0 - \frac{(\mu_i+\gamma)(\mu_e+\varepsilon)}{\varepsilon}I\\
&= -F_1F_2\frac{\mu_s}{S}\left(S-\bar{S}_0\right)^2 + \frac{(\mu_i+\gamma)(\mu_e+\varepsilon)}{\varepsilon}\left(\frac{F_1F_2\varepsilon\psi'(0)\bar{S}_0}{(\mu_i+\gamma)(\mu_e+\varepsilon)} - 1\right)I\\
&= -F_1F_2\frac{\mu_s}{S}\left(S-\bar{S}_0\right)^2 + \frac{(\mu_i+\gamma)(\mu_e+\varepsilon)}{\varepsilon}\left(\mathcal{R}_0^d - 1\right)I.
\end{aligned}$$

Therefore, for all $S, E, I, R > 0$ we have $\dfrac{d\mathcal{L}_1^d}{dt} \le 0$ when $\mathcal{R}_d \le 1$. Moreover, $\dfrac{d\mathcal{L}_1^d}{dt} = 0$ when $S = \bar{S}_0$ and $(\mathcal{R}_d - 1)I = 0$. According to [24], solutions of system (2.1) converge to the largest invariant subset of $\mathcal{M}_1^d = \left\{(S, E, I, R) \in \Omega^d : \dfrac{d\mathcal{L}_1^d}{dt} = 0\right\}$, which contains elements with $S(t) = \bar{S}_0$ and

$$(\mathcal{R}_d - 1)I = 0. \tag{4.7}$$

Let us consider two cases:

- If $\mathcal{R}_d < 1$, then from Eq (4.7), we obtain $I = 0$. Since $\mathcal{M}_1^d$ is invariant, we obtain $\dot{I}(t) = 0$. From the third equation of system (2.1) , we have

$$0 = \dot{I} = \varepsilon\int_0^{\omega_2}\Pi_2(\tau)E(t-\tau)d\tau = 0, \text{ for any } t, \tag{4.8}$$

so $E(t) = 0$ for all $t \geq 0$. Furthermore, since $I(t) \longrightarrow 0$, we use

$$R(t) = e^{-\mu_r t}\phi_4(0) + \gamma \int_0^t e^{-\mu_r(t-\theta)} \int_0^{\omega_3} \Pi_3(\tau) I(\theta - \tau)\, d\tau\, d\theta.$$

Since

$$\int_0^{\omega_3} \Pi_3(\tau) I(\theta - \tau)\, d\tau \longrightarrow 0,$$

the stability of the scalar linear equation implies

$$R(t) \longrightarrow 0.$$

Hence, $\mathcal{M}_1^d = \left\{\mathcal{E}_0^d\right\}$.

- If $\mathcal{R}_d = 1$, we have $S = \bar{S}_0$, and then $\dot{S}(t) = 0$. From the first equation of system (2.1), we have

$$\Lambda - \psi(I)S - \mu_s S = 0 \Longrightarrow \psi(I(t))\bar{S}_0 = 0, \text{ for any } t. \tag{4.9}$$

This implies that $I(t) = 0$ for all $t \geq 0$. As in the first case, from the third equation of system (2.1), we get $E(t) = 0$, for any t. Similarly, since $I = 0$, $\lim_{t\to\infty} R(t) = 0$. Hence, $\mathcal{M}_1^d = \left\{\mathcal{E}_0^d\right\}$.

LaSalle's invariance principle [25] reveals that $\mathcal{E}_0^d = \left(\bar{S}_0, 0, 0, 0\right)$ is GAS only if $\mathcal{R}_d \leq 1$. □

We next study the global stability of the endemic equilibrium when avian influenza persists in the bird population. Define the positive region

$$\Omega_2^d = \left\{(S, E, I, R) \in \mathbb{R}_+^4 : S > 0,\ E > 0,\ I > 0,\ R \geq 0\right\}.$$

Theorem 6. *If $\mathcal{R}_d > 1$, then the endemic equilibrium*

$$\mathcal{E}^* = (S^*, E^*, I^*, R^*)$$

is globally asymptotically stable.

Proof. Let

$$\varphi(x) = x - 1 - \ln x, \qquad x > 0.$$

Then $\varphi(x) \geq 0$, and equality holds if and only if $x = 1$. Consider the Lyapunov functional

$$\begin{aligned}\mathcal{L}_2^d(t) = {} & F_1F_2S^*\varphi\left(\frac{S(t)}{S^*}\right) + F_2E^*\varphi\left(\frac{E(t)}{E^*}\right) + \frac{(\mu_e+\varepsilon)}{\varepsilon}I^*\varphi\left(\frac{I(t)}{I^*}\right) \\ & + F_2\psi(I^*)S^* \int_0^{\omega_1} \Pi_1(\tau) \int_{t-\tau}^t \varphi\left(\frac{\psi(I(\theta))S(\theta)}{\psi(I^*)S^*}\right) d\theta\, d\tau \\ & + (\mu_e+\varepsilon)E^* \int_0^{\omega_2} \Pi_2(\tau) \int_{t-\tau}^t \varphi\left(\frac{E(\theta)}{E^*}\right) d\theta\, d\tau.\end{aligned}$$

This functional is non-negative for all positive solutions and vanishes, up to an additive constant, only at the endemic equilibrium.

Differentiating $\mathcal{L}_2^d$ along solutions of (2.1) gives

$$\begin{aligned}
\dot{\mathcal{L}}_2^d(t) &= F_1F_2\left(1-\frac{S^*}{S}\right)(\Lambda-\psi(I)S-\mu_sS)\\
&\quad+F_2\left(1-\frac{E^*}{E}\right)\left(\int_0^{\omega_1}\Pi_1(\tau)\psi(I^\tau)S^\tau\,d\tau-(\varepsilon+\mu_e)E\right)\\
&\quad+\frac{(\mu_e+\varepsilon)}{\varepsilon}\left(1-\frac{I^*}{I}\right)\left(\varepsilon\int_0^{\omega_2}\Pi_2(\tau)E^\tau\,d\tau-(\gamma+\mu_i)I\right)\\
&\quad+F_2\psi(I^*)S^*\int_0^{\omega_1}\Pi_1(\tau)\left[\frac{\psi(I)S}{\psi(I^*)S^*}-\frac{\psi(I^\tau)S^\tau}{\psi(I^*)S^*}+\ln\left(\frac{\psi(I^\tau)S^\tau}{\psi(I)S}\right)\right]d\tau\\
&\quad+(\mu_e+\varepsilon)E^*\int_0^{\omega_2}\Pi_2(\tau)\left[\frac{E}{E^*}-\frac{E^\tau}{E^*}+\ln\left(\frac{E^\tau}{E}\right)\right]d\tau\\
&=F_1F_2\left(1-\frac{S^*}{S}\right)(\Lambda-\mu_sS)-\frac{(\gamma+\mu_i)(\mu_e+\varepsilon)}{\varepsilon}I\left(1-\frac{I^*}{I}\right)\\
&\quad+F_2\psi(I^*)S^*\int_0^{\omega_1}\Pi_1(\tau)\left[\frac{\psi(I)}{\psi(I^*)}-\frac{\psi(I^\tau)S^\tau E^*}{\psi(I^*)S^*E}+\ln\left(\frac{\psi(I^\tau)S^\tau}{\psi(I)S}\right)\right]d\tau\\
&\quad+(\mu_e+\varepsilon)E^*\int_0^{\omega_2}\Pi_2(\tau)\left[1-\frac{E^\tau I^*}{E^*I}+\ln\left(\frac{E^\tau}{E}\right)\right]d\tau,
\end{aligned}$$

where, for simplicity, we have used

$$S^\tau=S(t-\tau),\qquad E^\tau=E(t-\tau),\qquad I^\tau=I(t-\tau).$$

At the endemic equilibrium, the following relations hold: $\Lambda=\mu_sS^*+\psi(I^*)S^*$, $F_1\psi(I^*)S^*=(\mu_e+\varepsilon)E^*$, and $\varepsilon F_2E^*=(\mu_i+\gamma)I^*$. Then $\frac{(\gamma+\mu_i)(\mu_e+\varepsilon)}{\varepsilon}I^*=F_1F_2\psi(I^*)S^*$. Using these identities and simplifying, we obtain

$$\begin{aligned}
\dot{\mathcal{L}}_2^d(t) &= F_1F_2\left(1-\frac{S^*}{S}\right)(\mu_sS^*+\psi(I^*)S^*-\mu_sS)-F_1F_2\psi(I^*)S^*\left(\frac{I}{I^*}-1\right)\\
&\quad+F_2\psi(I^*)S^*\int_0^{\omega_1}\Pi_1(\tau)\left[\frac{\psi(I)}{\psi(I^*)}-\frac{\psi(I^\tau)S^\tau E^*}{\psi(I^*)S^*E}+\ln\left(\frac{\psi(I^\tau)S^\tau}{\psi(I)S}\right)\right]d\tau\\
&\quad+F_1\psi(I^*)S^*\int_0^{\omega_2}\Pi_2(\tau)\left[1-\frac{E^\tau I^*}{E^*I}+\ln\left(\frac{E^\tau}{E}\right)\right]d\tau\\
&=-\mu_sF_1F_2\frac{(S-S^*)^2}{S}+F_1F_2\psi(I^*)S^*\left(1-\frac{S^*}{S}\right)+F_1F_2\psi(I^*)S^*\left(1-\frac{I}{I^*}\right)\\
&\quad+F_2\psi(I^*)S^*\int_0^{\omega_1}\Pi_1(\tau)\left[1-\frac{\psi(I^\tau)S^\tau E^*}{\psi(I^*)S^*E}+\ln\left(\frac{\psi(I^\tau)S^\tau E^*}{\psi(I^*)S^*E}\right)\right]d\tau\\
&\quad+F_2\psi(I^*)S^*\int_0^{\omega_1}\Pi_1(\tau)\left[\frac{\psi(I)}{\psi(I^*)}-1+\ln\left(\frac{\psi(I^\tau)S^\tau}{\psi(I)S}\right)-\ln\left(\frac{\psi(I^\tau)S^\tau E^*}{\psi(I^*)S^*E}\right)\right]d\tau\\
&\quad+F_1\psi(I^*)S^*\int_0^{\omega_2}\Pi_2(\tau)\left[1-\frac{E^\tau I^*}{E^*I}+\ln\left(\frac{E^\tau I^*}{E^*I}\right)\right]d\tau\\
&\quad+F_1\psi(I^*)S^*\int_0^{\omega_2}\Pi_2(\tau)\left[\ln\left(\frac{E^\tau}{E}\right)-\ln\left(\frac{E^\tau I^*}{E^*I}\right)\right]d\tau
\end{aligned}$$

$$
\begin{aligned}
&= -\mu_s F_1 F_2 \frac{(S - S^*)^2}{S} + F_1 F_2 \psi(I^*) S^* \left(1 - \frac{S^*}{S}\right) + F_1 F_2 \psi(I^*) S^* \left(1 - \frac{I}{I^*}\right) \\
&\quad + F_2 \psi(I^*) S^* \int_0^{\omega_1} \Pi_1(\tau) \left[1 - \frac{\psi(I^\tau) S^\tau E^*}{\psi(I^*) S^* E} + \ln\left(\frac{\psi(I^\tau) S^\tau E^*}{\psi(I^*) S^* E}\right)\right] d\tau \\
&\quad + F_1 F_2 \psi(I^*) S^* \left[\frac{\psi(I)}{\psi(I^*)} - 1 + \ln\left(\frac{\psi(I^*) S^* E}{\psi(I) S E^*}\right)\right] + F_1 F_2 \psi(I^*) S^* \ln\left(\frac{E^* I}{E I^*}\right) \\
&\quad + F_1 \psi(I^*) S^* \int_0^{\omega_2} \Pi_2(\tau) \left[1 - \frac{E^\tau I^*}{E^* I} + \ln\left(\frac{E^\tau I^*}{E^* I}\right)\right] d\tau \\
&= -\mu_s F_1 F_2 \frac{(S - S^*)^2}{S} + F_2 \psi(I^*) S^* \int_0^{\omega_1} \Pi_1(\tau) \left[1 - \frac{\psi(I^\tau) S^\tau E^*}{\psi(I^*) S^* E} + \ln\left(\frac{\psi(I^\tau) S^\tau E^*}{\psi(I^*) S^* E}\right)\right] d\tau \\
&\quad + F_1 \psi(I^*) S^* \int_0^{\omega_2} \Pi_2(\tau) \left[1 - \frac{E^\tau I^*}{E^* I} + \ln\left(\frac{E^\tau I^*}{E^* I}\right)\right] d\tau \\
&\quad + F_1 F_2 \psi(I^*) S^* \left[1 - \frac{S^*}{S} - \frac{I}{I^*} + \frac{\psi(I)}{\psi(I^*)} + \ln\left(\frac{\psi(I^*) S^* I}{\psi(I) S I^*}\right)\right] \\
&= -\mu_s F_1 F_2 \frac{(S - S^*)^2}{S} + F_1 F_2 \psi(I^*) S^* \left[1 - \frac{S^*}{S} - \frac{I}{I^*} + \frac{\psi(I)}{\psi(I^*)} + \ln\left(\frac{\psi(I^*) S^* I}{\psi(I) S I^*}\right)\right] \\
&\quad - F_2 \psi(I^*) S^* \int_0^{\omega_1} \Pi_1(\tau) \varphi\left(\frac{\psi(I^\tau) S^\tau E^*}{\psi(I^*) S^* E}\right) d\tau - F_1 \psi(I^*) S^* \int_0^{\omega_2} \Pi_2(\tau) \varphi\left(\frac{E^\tau I^*}{E^* I}\right) d\tau \\
&= -\mu_s F_1 F_2 \frac{(S - S^*)^2}{S} - F_1 F_2 \psi(I^*) S^* \varphi\left(\frac{S^*}{S}\right) \\
&\quad - F_2 \psi(I^*) S^* \int_0^{\omega_1} \Pi_1(\tau) \varphi\left(\frac{\psi(I^\tau) S^\tau E^*}{\psi(I^*) S^* E}\right) d\tau - F_1 \psi(I^*) S^* \int_0^{\omega_2} \Pi_2(\tau) \varphi\left(\frac{E^\tau I^*}{E^* I}\right) d\tau \\
&\quad + F_1 F_2 \psi(I^*) S^* \left[-\frac{I}{I^*} + \ln\left(\frac{I}{I^*}\right) + \frac{\psi(I)}{\psi(I^*)} - \ln\left(\frac{\psi(I)}{\psi(I^*)}\right)\right].
\end{aligned}
$$

Since $\varphi(x) \geq 0$ for all $x > 0$, the integral terms and the second term are non-positive. In addition,

$$-\mu_s F_1 F_2 \frac{(S - S^*)^2}{S} \leq 0.$$

It remains to be shown that the last term is non-positive. Set $x = \dfrac{I}{I^*}$, $y = \dfrac{\psi(I)}{\psi(I^*)}$, and $f(t) = t - \ln t$. Then

$$\left[-\frac{I}{I^*} + \ln\left(\frac{I}{I^*}\right) + \frac{\psi(I)}{\psi(I^*)} - \ln\left(\frac{\psi(I)}{\psi(I^*)}\right)\right] = f(y) - f(x).$$

Since $f'(t) = 1 - \dfrac{1}{t}$, the function f is strictly decreasing on $(0, 1)$ and strictly increasing on $(1, \infty)$, with a global minimum $f(1) = 1$.

Because ψ is concave and increasing with $\psi(0) \geq 0$, the function $I \mapsto \psi(I)/I$ is decreasing. Hence

$$I > I^* \implies y < x, \qquad I < I^* \implies y > x.$$

Moreover, since ψ is increasing,

$$I > I^* \implies x > 1,\ y > 1, \qquad I < I^* \implies x < 1,\ y < 1.$$

Thus, x and y always lie on the same side of 1, and y is closer to 1 than x is.

- If $I > I^*$, then $1 < y < x$. Since f is increasing on $(1, \infty)$,

$$f(y) < f(x) \implies \left[-\frac{I}{I^*} + \ln\left(\frac{I}{I^*}\right) + \frac{\psi(I)}{\psi(I^*)} - \ln\left(\frac{\psi(I)}{\psi(I^*)}\right)\right] < 0.$$

- If $I < I^*$, then $0 < x < y < 1$. Since f is decreasing on $(0, 1)$,

$$f(y) < f(x) \implies \left[-\frac{I}{I^*} + \ln\left(\frac{I}{I^*}\right) + \frac{\psi(I)}{\psi(I^*)} - \ln\left(\frac{\psi(I)}{\psi(I^*)}\right)\right] < 0.$$

- If $I = I^*$, then $x = y = 1$, so $\left[-\frac{I}{I^*} + \ln\left(\frac{I}{I^*}\right) + \frac{\psi(I)}{\psi(I^*)} - \ln\left(\frac{\psi(I)}{\psi(I^*)}\right)\right] = 0.$

Consequently,

$$\dot{\mathcal{L}}_2^d(t) \leq 0$$

for all positive solutions in Ω_2^d.

It remains to determine the largest invariant set contained in

$$\mathcal{M}_2^d = \left\{(S, E, I, R) \in \Omega_2^d : \dot{\mathcal{L}}_2^d(t) = 0\right\}.$$

The equality $\dot{\mathcal{L}}_2^d(t) = 0$ holds only when

$$S(t) = S^*, \qquad I(t) = I^*,$$

and

$$\frac{\psi(I(t-\tau))S(t-\tau)E^*}{\psi(I^*)S^*E(t)} = 1, \qquad \frac{E(t-\tau)I^*}{E^*I(t)} = 1,$$

for almost every τ in the corresponding delay intervals. These relations imply, on the largest invariant set, that

$$E(t) = E^*, \qquad I(t) = I^*.$$

The recovered component is not inferred directly from $\dot{\mathcal{L}}_2^d = 0$. Instead, using

$$\dot{R}(t) = \gamma \int_0^{\omega_3} \Pi_3(\tau) I(t-\tau)\, d\tau - \mu_r R(t)$$

and $I(t) \to I^*$, we obtain

$$R(t) = e^{-\mu_r t}\phi_4(0) + \gamma \int_0^t e^{-\mu_r(t-\theta)} \int_0^{\omega_3} \Pi_3(\tau) I(\theta-\tau)\, d\tau\, d\theta,$$

and therefore

$$\lim_{t\to\infty} R(t) = \frac{\gamma F_3}{\mu_r} I^* = R^*.$$

Thus, the largest invariant subset of $\mathcal{M}_2^d$ is the singleton $\{\mathcal{E}^*\}$. By LaSalle's invariance principle for functional differential equations [26], every positive solution of (2.1) approaches $\mathcal{E}^*$ as $t \to \infty$. Therefore, the endemic equilibrium is globally asymptotically stable whenever $\mathcal{R}_d > 1$. □

5. Numerical simulations

In this section, numerical simulations are carried out to illustrate the theoretical results obtained for the avian influenza model. The simulations are used to compare the non-delayed system (3.1) with the delayed system (2.1) and to examine how the threshold quantity influences the persistence or elimination of infection in the bird population. For numerical implementation, the distributed-delay terms are approximated by Dirac delta functions centered at fixed delay values [27–29]. More precisely, we take

$$\zeta_i(\tau) = \delta(\tau - \tau_i), \qquad i = 1, 2, 3,$$

where τ_i denotes the corresponding discrete delay. In this case,

$$\int_0^\infty \zeta_i(\tau)\, d\tau = 1,$$

and the survival factors become

$$F_i = \int_0^\infty \delta(\tau - \tau_i) e^{-n_i\tau}\, d\tau = e^{-n_i\tau_i}, \qquad i = 1, 2, 3.$$

Consequently, the distributed-delay terms reduce to

$$\int_0^\infty \delta(\tau - \tau_1) e^{-n_1\tau} \psi(I(t-\tau)) S(t-\tau)\, d\tau = e^{-n_1\tau_1} \psi(I(t-\tau_1)) S(t-\tau_1),$$

$$\int_0^\infty \delta(\tau - \tau_2) e^{-n_2\tau} E(t-\tau)\, d\tau = e^{-n_2\tau_2} E(t-\tau_2),$$

and

$$\int_0^\infty \delta(\tau - \tau_3) e^{-n_3\tau} I(t-\tau)\, d\tau = e^{-n_3\tau_3} I(t-\tau_3).$$

Thus, the distributed-delay model (2.1) is converted into the following fixed-delay system:

$$\begin{cases} \dot{S}(t) &= \Lambda - \psi(I(t))S(t) - \mu_s S(t), \\ \dot{E}(t) &= e^{-n_1\tau_1}\psi(I(t-\tau_1))S(t-\tau_1) - (\varepsilon + \mu_e)E(t), \\ \dot{I}(t) &= \varepsilon e^{-n_2\tau_2} E(t-\tau_2) - (\gamma + \mu_i) I(t), \\ \dot{R}(t) &= \gamma e^{-n_3\tau_3} I(t-\tau_3) - \mu_r R(t). \end{cases} \tag{5.1}$$

For system (5.1), the delayed basic reproduction number is given by

$$\mathcal{R}_d = \frac{\varepsilon \Lambda e^{-n_1\tau_1 - n_2\tau_2} \psi'(0)}{\mu_s(\mu_e + \varepsilon)(\mu_i + \gamma)}.$$

This expression shows that the first two delay periods, together with the survival factors $e^{-n_1\tau_1}$ and $e^{-n_2\tau_2}$, directly affect the ability of avian influenza to invade the bird population.

The non-delayed system (3.1) is solved numerically using the `ode45` solver in MATLAB, while the fixed-delay system (5.1) is solved using the `dde23` solver. Unless otherwise stated, we choose

$$n_i = 1, \qquad \tau_i = 0.1, \qquad i = 1, 2, 3.$$

For the nonlinear incidence rate, we use the Monod-type saturated function

$$\psi(I) = \frac{\eta I}{\kappa + I},$$

where $\eta > 0$ represents the maximum transmission rate and $\kappa > 0$ controls the saturation level. This function is non-negative, increasing, bounded, and concave for $I \geq 0$, and it satisfies

$$\psi(0) = 0, \qquad \psi'(0) = \frac{\eta}{\kappa}.$$

The parameter values used in the numerical experiments are listed in Table 2. These values are selected to illustrate the qualitative behavior predicted by the theoretical analysis, including disease extinction when the reproduction number is below unity and disease persistence when it is above unity.

Table 2. Parameter values used in the numerical simulations of the avian influenza model.

Parameter	Value	Units	Biological justification
κ	4	Individuals	Saturation constant
μ_s	0.6	1/time	Natural mortality of susceptible birds
μ_e	0.9	1/time	Mortality of exposed birds
μ_i	0.4	1/time	Mortality/removal of infectious birds
μ_r	0.3	1/time	Mortality of recovered birds
ε	1.1	1/time	Progression rate from exposed to infectious
γ	0.4	1/time	Recovery rate of infectious birds

These values fall within biologically plausible ranges for avian influenza transmission in bird populations. For instance, the mortality rates $(\mu_s, \mu_e, \mu_i, \mu_r)$ are consistent with typical lifespans of domestic poultry, and the progression rate ε and recovery rate γ align with estimates from avian influenza epidemiology studies. The saturation parameter κ and the maximum transmission rate η are chosen to demonstrate both disease extinction (when $\mathcal{R}_0 \leq 1$) and disease persistence (when $\mathcal{R}_0 > 1$) scenarios.

5.1. Numerical dynamics without distributed delays

We first illustrate the behavior of the non-delayed avian influenza model (3.1). The simulations are performed for several initial bird populations in order to verify that the long-term behavior of the system is determined by the basic reproduction number $\mathcal{R}_0$ and not by the particular choice of initial data.

Figure 2 corresponds to the case $\mathcal{R}_0 = 0.859 < 1$, obtained by taking $\eta = 1$ and $\Lambda = 3$. In this situation, each infectious bird generates less than one new infection on average, and the virus cannot be sustained in the bird population. The numerical trajectories show that the exposed and infectious classes decay to zero, while the recovered class also vanishes gradually due to mortality. At the same time, the susceptible bird population approaches its disease-free level. Thus, all solution curves converge to

$$\mathcal{E}_0 = \left(\frac{\Lambda}{\mu_s}, 0, 0, 0\right) = (5, 0, 0, 0),$$

which supports the theoretical result that the disease-free equilibrium is globally asymptotically stable when $\mathcal{R}_0 \leq 1$.

Figure 3 describes the case $\mathcal{R}_0 = 11.4583 > 1$, with $\eta = 2.5$ and $\Lambda = 16$. Here, the transmission potential is sufficiently high for avian influenza to persist in the bird population. The simulations show a different pattern from the disease-free case: Although the solutions start from distinct initial conditions and may initially increase or decrease, all trajectories eventually settle at the same positive steady state. In particular, the susceptible, exposed, infectious, and recovered bird classes converge to the endemic equilibrium

$$\mathcal{E}^* = (7.038, 5.889, 8.097, 10.796).$$

This numerical behavior confirms the analytical result that the endemic equilibrium is globally asymptotically stable whenever $\mathcal{R}_0 > 1$.

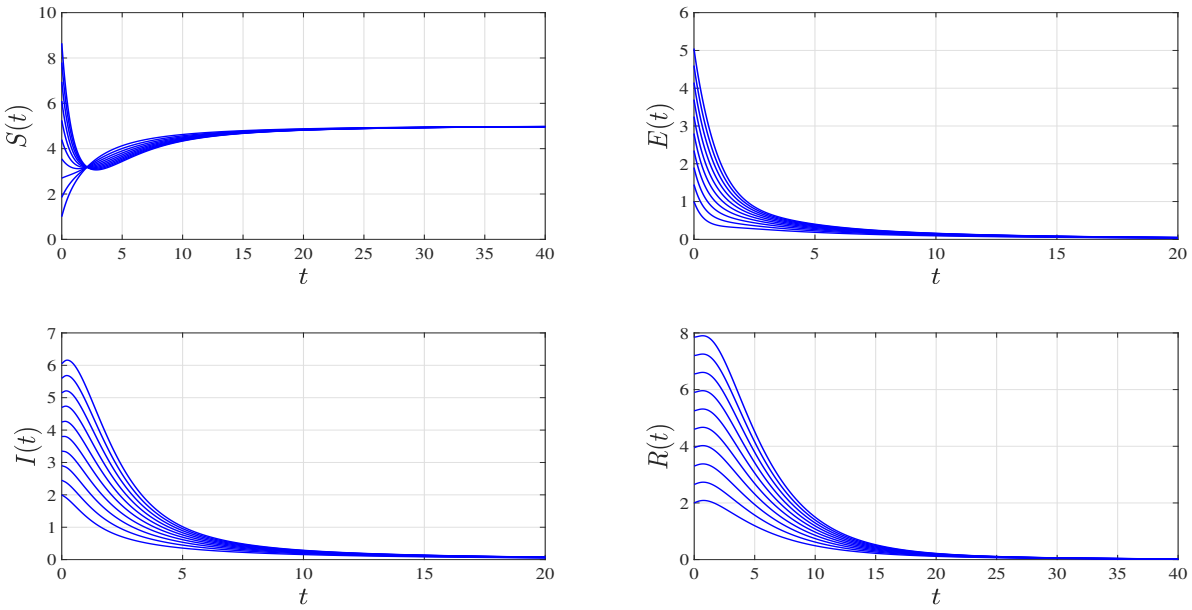


Figure 2. Numerical solutions of the non-delayed avian influenza model (3.1) for different initial bird populations when $\mathcal{R}_0 = 0.859 < 1$.

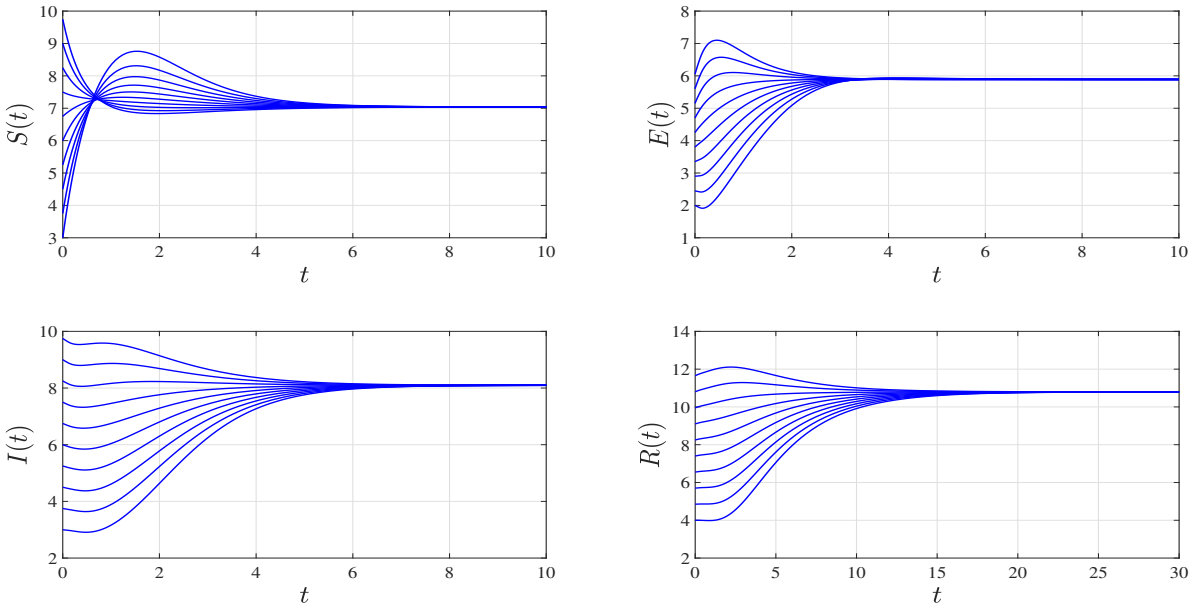


Figure 3. Numerical solutions of the non-delayed avian influenza model (3.1) for different initial bird populations when $\mathcal{R}_0 = 11.4583 > 1$.

5.2. Numerical dynamics with distributed delays

We now illustrate the behavior of the delayed avian influenza model (5.1). In contrast to the non-delayed case, the transitions from effective exposure to the exposed class, from the exposed class to the infectious class, and from the infectious class to the recovered class are affected by the delay terms. The simulations are carried out for different initial conditions in order to examine whether the long-term dynamics remain consistent with the theoretical threshold results established for $\mathcal{R}_d$.

Figure 4 corresponds to the case $\mathcal{R}_d = 0.704 < 1$, with $\eta = 1$ and $\Lambda = 3$. In this case, the delayed reproduction number is below unity, meaning that avian influenza cannot persist in the bird population. The numerical trajectories show that the exposed and infectious bird classes decrease to zero, while the recovered class also vanishes over time. The susceptible class approaches the disease-free level $\frac{\Lambda}{\mu_s} = 5$. Although the presence of delays produces transient changes in the trajectories, all solutions ultimately converge to the disease-free equilibrium

$$\mathcal{E}_0 = (5, 0, 0, 0).$$

This supports the theoretical result that $\mathcal{E}_0$ is globally asymptotically stable whenever $\mathcal{R}_d \leq 1$.

Figure 5 presents the case $\mathcal{R}_d = 9.381 > 1$, with $\eta = 2.5$ and $\Lambda = 16$. Here, the delayed reproduction number is greater than one, indicating that avian influenza can establish itself in the bird population. The numerical solutions show a clear endemic pattern: starting from different initial conditions, the susceptible, exposed, infectious, and recovered classes all approach the same positive steady state. The delay terms produce visible transient effects, particularly in the exposed and infectious classes, where the trajectories may initially rise or fall before settling. Nevertheless, the long-term behavior is stable and all solutions converge to

$$\mathcal{E}^* = (7.454, 5.215, 6.489, 7.828).$$

This confirms the analytical result that the endemic equilibrium is globally asymptotically stable when $\mathcal{R}_d > 1$.

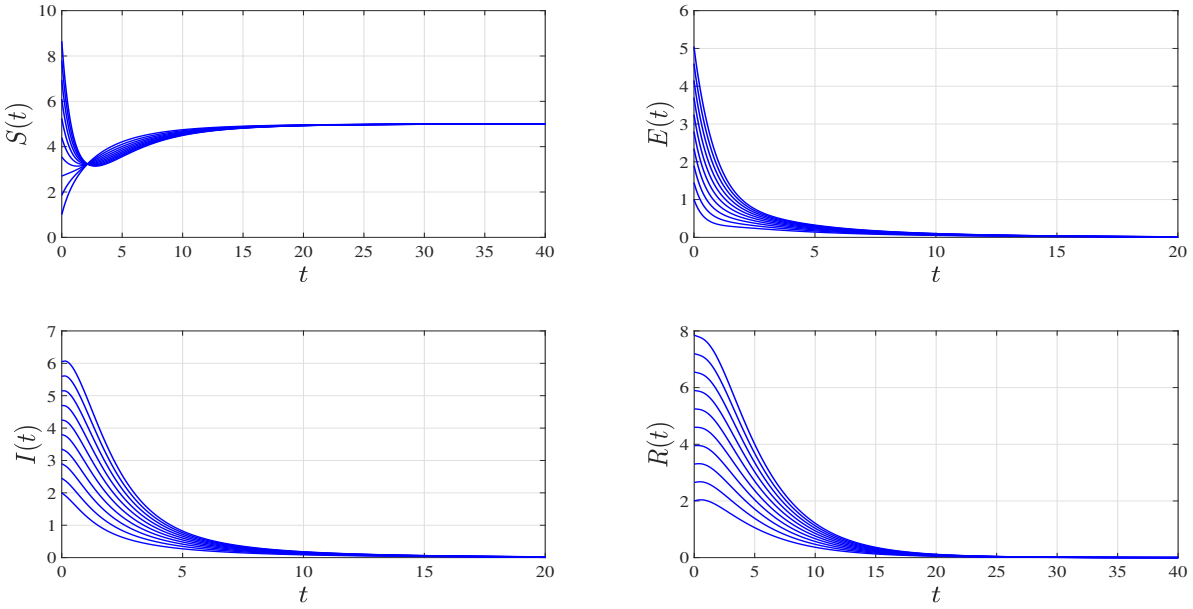


Figure 4. Numerical solutions of the delayed avian influenza model (5.1) for different initial conditions when $\mathcal{R}_d = 0.704 < 1$.

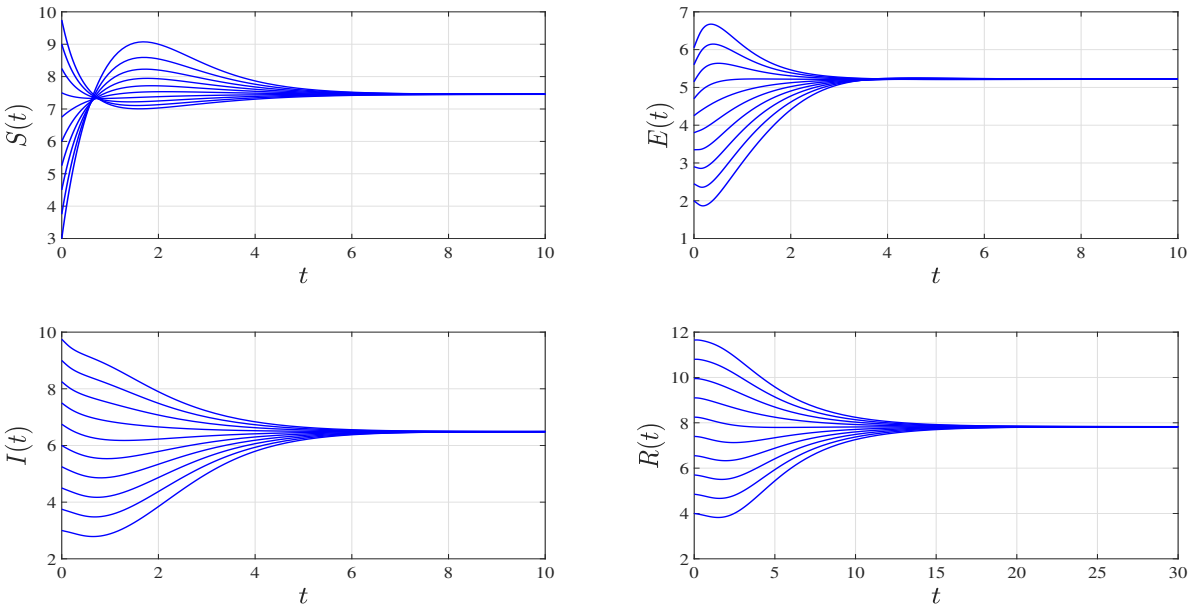


Figure 5. Numerical solutions of the delayed avian influenza model (5.1) for different initial conditions when $\mathcal{R}_d = 9.381 > 1$.

5.3. Sensitivity analysis

To identify the parameters that have the greatest influence on avian influenza transmission in the delayed bird model, we perform a normalized sensitivity analysis of the delayed basic reproduction number $\mathcal{R}_d$. This type of analysis measures how a relative change in a model parameter affects the relative change in $\mathcal{R}_d$ [30,31]. In the present setting, the results are useful for identifying the biological and epidemiological processes that most strongly promote or reduce the spread of avian influenza in the bird population. A positive sensitivity index indicates that increasing the corresponding parameter increases $\mathcal{R}_d$, whereas a negative index means that increasing the parameter decreases $\mathcal{R}_d$.

Definition 1 (Normalized forward sensitivity index)**.** *Let ρ be a parameter appearing in $\mathcal{R}_d$. The normalized forward sensitivity index of $\mathcal{R}_d$ with respect to ρ is defined by*

$$\Upsilon_{\rho}^{\mathcal{R}_d} = \frac{\partial \mathcal{R}_d}{\partial \rho}\frac{\rho}{\mathcal{R}_d}.$$

The normalized sensitivity index $\Upsilon_{\rho}^{R_d} = \dfrac{\partial R_d}{\partial \rho}\dfrac{\rho}{R_d}$ measures the local relative response of the reproduction number to a relative perturbation of the parameter ρ. For a sufficiently small relative perturbation $\Delta\rho/\rho$, one has the first-order approximation $\dfrac{\Delta R_d}{R_d} \approx \Upsilon_{\rho}^{R_d}\dfrac{\Delta\rho}{\rho}$. Thus, the sensitivity index should be interpreted as a local elasticity rather than as an exact percentage response to a finite, particularly 100%, parameter change. For nonlinear dependence, finite changes should instead be evaluated directly from the expression for R_d or through a global sensitivity analysis.

For the delayed avian influenza model, the basic reproduction number is given by

$$\mathcal{R}_d = \frac{\varepsilon\Lambda e^{-n_1\tau_1 - n_2\tau_2}\psi'(0)}{\mu_s(\mu_i+\gamma)(\mu_e+\varepsilon)}.$$

Using Definition 1, the sensitivity indices of $\mathcal{R}_d$ are listed in Table 3.

Table 3 and Figure 6(a) show that the recruitment rate of susceptible birds, Λ, has the strongest positive effect on $\mathcal{R}_d$. In epidemiological terms, increasing the inflow of susceptible birds into the population increases the number of birds available for infection and therefore raises the transmission potential of avian influenza. The progression rate from the exposed class to the infectious class, ε, also has a positive effect. This indicates that faster movement of exposed birds into the infectious class increases the expected number of secondary infections. On the other hand, the mortality rate of susceptible birds, μ_s, has the largest negative effect, with sensitivity index -1. Thus, a 100% increase in μ_s produces a 100% decrease in $\mathcal{R}_d$, assuming all other parameters remain fixed. The infectious-bird mortality/removal rate μ_i and the recovery rate γ have moderate negative effects, each with sensitivity index -0.50. This means that increasing either of these parameters by 100% reduces $\mathcal{R}_d$ by approximately 50%. Similarly, increasing the exposed-bird mortality rate μ_e by 100% reduces $\mathcal{R}_d$ by about 45%.

Table 3. Normalized sensitivity indices of $\mathcal{R}_d$ for the delayed avian influenza model.

Parameter	Sensitivity index	Value	Effect
Λ	$\Upsilon_{\Lambda}^{\mathcal{R}_d} = 1$	1	Positive
ε	$\Upsilon_{\varepsilon}^{\mathcal{R}_d} = \dfrac{\mu_e}{\mu_e + \varepsilon}$	0.45	Positive
n_1	$\Upsilon_{n_1}^{\mathcal{R}_d} = -n_1\tau_1$	-0.10	Negative
τ_1	$\Upsilon_{\tau_1}^{\mathcal{R}_d} = -n_1\tau_1$	-0.10	Negative
n_2	$\Upsilon_{n_2}^{\mathcal{R}_d} = -n_2\tau_2$	-0.10	Negative
τ_2	$\Upsilon_{\tau_2}^{\mathcal{R}_d} = -n_2\tau_2$	-0.10	Negative
μ_e	$\Upsilon_{\mu_e}^{\mathcal{R}_d} = -\dfrac{\mu_e}{\mu_e + \varepsilon}$	-0.45	Negative
μ_i	$\Upsilon_{\mu_i}^{\mathcal{R}_d} = -\dfrac{\mu_i}{\mu_i + \gamma}$	-0.50	Negative
γ	$\Upsilon_{\gamma}^{\mathcal{R}_d} = -\dfrac{\gamma}{\mu_i + \gamma}$	-0.50	Negative
μ_s	$\Upsilon_{\mu_s}^{\mathcal{R}_d} = -1$	-1	Negative

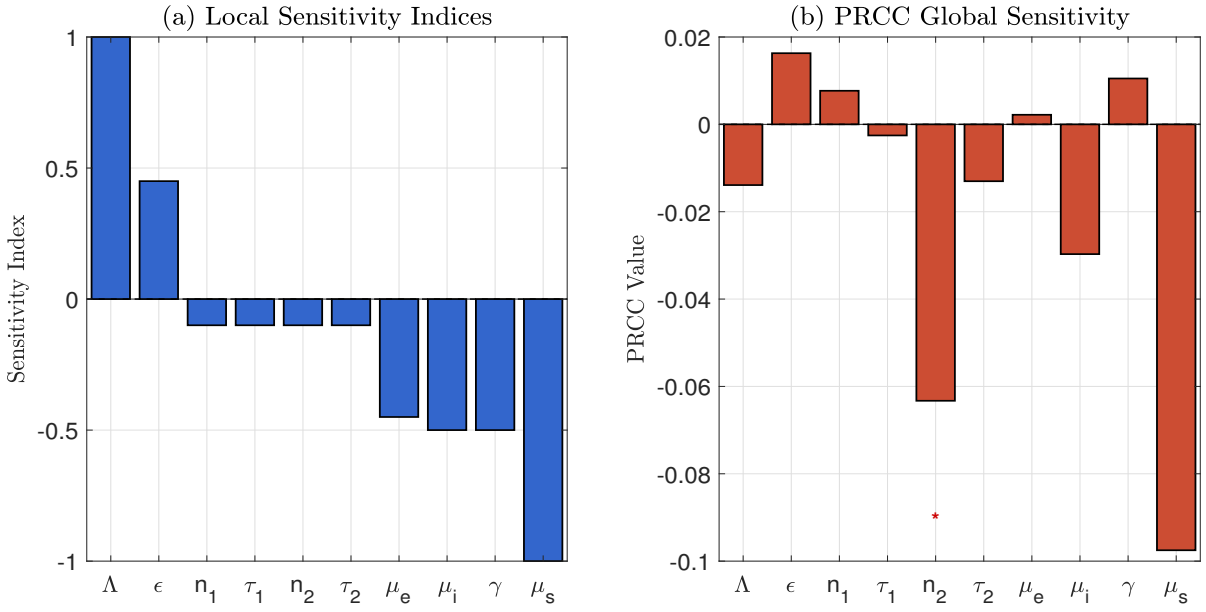


Figure 6. Local sensitivity indices and PRCC values of $\mathcal{R}_d$ with respect to the main parameters of the delayed avian influenza model.

To complement the local sensitivity analysis, we perform a global sensitivity analysis using the partial rank correlation coefficient (PRCC) method [32–35]. Unlike the local sensitivity indices, which measure the effect of small perturbations around a nominal parameter value, PRCC assesses the overall impact of each parameter across its entire plausible range while accounting for correlations among parameters.

For the PRCC analysis, we define uniform distributions for the key parameters over biologically plausible ranges (see Table 4):

Table 4. Parameter ranges for PRCC global sensitivity analysis.

Parameter	Λ	ϵ	μ_s	μ_e	μ_i	γ	τ_1	τ_2	n_1	n_2
Min	1	0.5	0.3	0.5	0.2	0.2	0.01	0.01	0.5	0.5
Max	20	2.0	0.9	1.5	0.8	0.8	0.5	0.5	2.0	2.0

We generate 1000 parameter sets using Latin hypercube sampling and compute $\mathcal{R}_d$ for each set. The PRCC values are then calculated to rank the parameters by their influence on $\mathcal{R}_d$.

Figure 6(b) presents the PRCC results alongside the local sensitivity indices. The PRCC analysis confirms that the recruitment rate of susceptible birds Λ has the strongest positive influence on $\mathcal{R}_d$, while the susceptible mortality rate μ_s has the strongest negative influence. The progression rate ϵ and the recovery rate γ also show significant effects. The delay parameters τ_1, τ_2, n_1, and n_2 have smaller but non-negligible effects on $\mathcal{R}_d$.

The agreement between the local and global sensitivity analyses strengthens our confidence in identifying the key parameters that determine whether avian influenza persists or dies out in the bird population. From a control perspective, interventions targeting Λ (e.g., reducing recruitment through biosecurity) or μ_s (e.g., culling susceptible birds) would have the greatest impact on reducing the reproduction number.

The delay-related parameters n_1, τ_1, n_2, and τ_2 have smaller negative sensitivity indices, each equal to -0.10 for the parameter values used in the simulations. These results suggest that increasing the duration of the delay or the mortality/removal rate during the delayed stages reduces the probability that infected birds survive long enough to contribute to new infections. Although their individual effects are weaker than those of Λ, μ_s, μ_i, and γ, the delay parameters still contribute to lowering the transmission potential by reducing survival through the exposed and infectious formation periods.

Hence, the sensitivity results indicate that $\mathcal{R}_d$ is most strongly influenced by the susceptible recruitment rate Λ and the susceptible mortality rate μ_s, followed by the infectious-bird mortality/removal rate μ_i, the recovery rate γ, the exposed-to-infectious progression rate ε, and the exposed-bird mortality rate μ_e. From a control perspective, the results emphasize the importance of reducing the number of susceptible birds exposed to infection, shortening the infectious period through rapid detection and removal of infectious birds, and limiting the survival of infection through the delayed transmission stages. The parameters τ_3, n_3, and μ_r do not appear in $\mathcal{R}_d$ and therefore do not affect the initial invasion threshold, although they may influence the size of the recovered class after infection has occurred.

If the Monod incidence function $\psi(I) = \dfrac{\eta I}{\kappa + I}$ is used, then $\psi'(0) = \dfrac{\eta}{\kappa}$. In this case, $\mathcal{R}_d$ is positively sensitive to the maximum transmission parameter η and negatively sensitive to the saturation parameter κ, with $\Upsilon_\eta^{\mathcal{R}_d} = 1$ and $\Upsilon_\kappa^{\mathcal{R}_d} = -1$.

5.4. Influence of infection-blocking control

In this subsection, we examine how an infection-blocking intervention affects the delayed avian influenza dynamics in birds. Since vaccination is not included in the present framework, the

parameter $p \in [0, 1]$ is introduced to represent the efficacy of a control measure that reduces effective transmission. This parameter may be interpreted as the combined effect of protective intervention, improved biosecurity, rapid separation of infected birds, or any measure that reduces the probability that a susceptible bird becomes infected after effective contact with infectious birds. Thus, $p = 0$ corresponds to the absence of such control, while $p = 1$ represents complete blocking of transmission. The controlled delayed model is given by

$$\begin{cases} \dot{S}(t) &= \Lambda - (1-p)\psi(I(t))S(t) - \mu_s S(t), \\ \dot{E}(t) &= (1-p)e^{-n_1\tau_1}\psi(I(t-\tau_1))S(t-\tau_1) - (\varepsilon + \mu_e)E(t), \\ \dot{I}(t) &= \varepsilon e^{-n_2\tau_2}E(t-\tau_2) - (\gamma + \mu_i)I(t), \\ \dot{R}(t) &= \gamma e^{-n_3\tau_3}I(t-\tau_3) - \mu_r R(t). \end{cases} \tag{5.2}$$

The corresponding controlled reproduction number is

$$\mathcal{R}_d^c(p) = (1-p)\mathcal{R}_d.$$

Hence, the control measure reduces the transmission potential of avian influenza in direct proportion to its efficacy. If the uncontrolled delayed system satisfies $\mathcal{R}_d > 1$, then the critical efficacy required to bring the reproduction number below the threshold value is determined from $\mathcal{R}_d^c(p^{cr}) = 1$. Therefore, $p^{cr} = 1 - \dfrac{1}{\mathcal{R}_d}$. Consequently, $\mathcal{R}_d^c(p) \leq 1$ whenever $p^{cr} \leq p \leq 1$.

In this case, the infection is expected to die out and the disease-free equilibrium becomes globally asymptotically stable. Using the parameter values adopted in the numerical simulations, we obtain $p^{cr} = 0.8477$. Thus, two epidemiological regimes can be distinguished:

$$0.8477 \leq p \leq 1 \quad \Longrightarrow \quad \mathcal{R}_d^c(p) \leq 1,$$

so that avian influenza is eliminated from the bird population, whereas

$$0 \leq p < 0.8477 \quad \Longrightarrow \quad \mathcal{R}_d^c(p) > 1,$$

so that infection may persist and the endemic equilibrium remains stable.

The values of $\mathcal{R}_d^c(p)$ for selected control efficacies are given in Table 5. The table shows that increasing p steadily lowers the controlled reproduction number. In particular, when $p = 0.7$, the value $\mathcal{R}_d^c(p) = 1.9701$ remains above unity, and control is insufficient to eliminate infection. As p increases toward the critical value $p^{cr} = 0.8477$, the reproduction number approaches one. For stronger control, such as $p = 0.95$, the reproduction number falls well below unity, indicating that avian influenza cannot be maintained in the bird population.

Table 5. Variation of the controlled reproduction number $\mathcal{R}_d^c(p)$ with respect to the control efficacy p.

Control efficacy p	$\mathcal{R}_d^c(p)$
0.70	1.9701
0.75	1.6417
0.80	1.3134
0.8477	1.0000
0.95	0.3283

Figure 7 illustrates the effect of increasing the control efficacy p on the four bird classes. The susceptible population increases as p becomes larger because fewer susceptible birds are converted into exposed birds. In contrast, the exposed and infectious classes decrease as the infection-blocking efficacy improves. This decrease is most pronounced when $p = 0.95$, where the controlled reproduction number is below unity and the infection is driven toward extinction. The recovered class also declines for larger values of p, which is expected because fewer birds become infected and therefore fewer birds enter the recovered class. Overall, the figure confirms that a sufficiently strong reduction of effective transmission can move the system from an endemic regime to a disease-free regime.

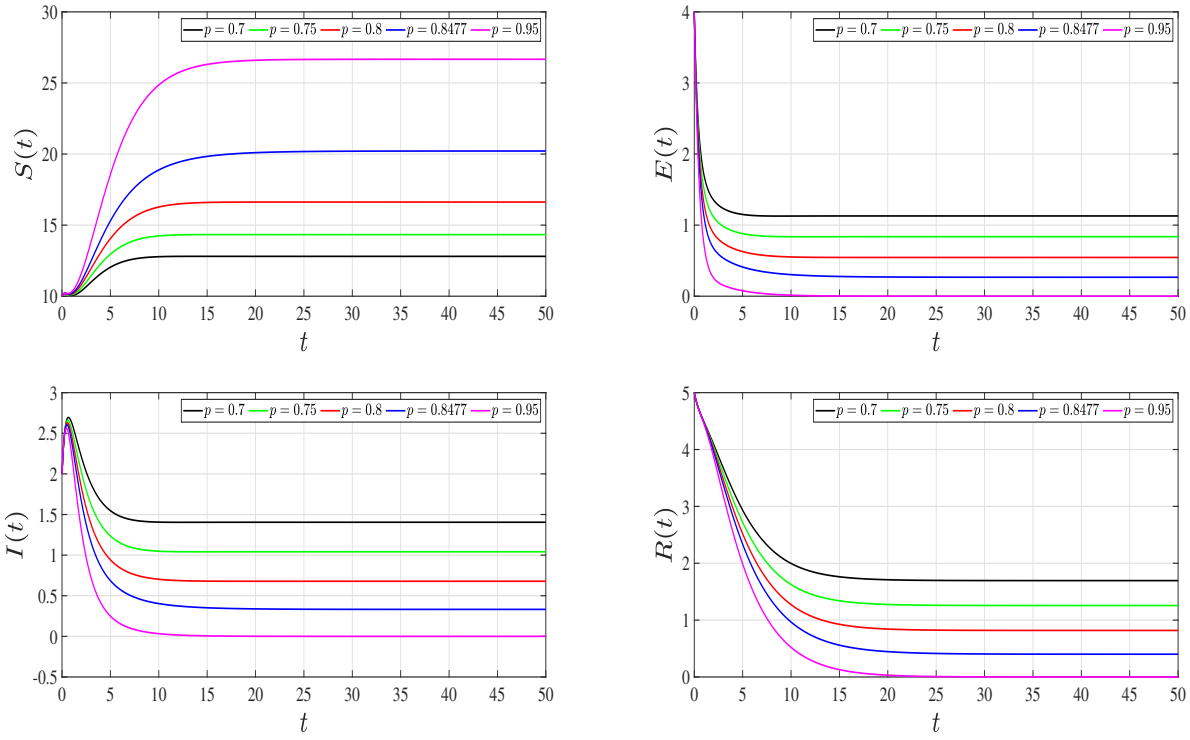


Figure 7. Effect of infection-blocking control efficacy p on the four bird classes in the delayed avian influenza model.

5.5. *Effect of time delays on system dynamics*

To investigate whether the time delays can induce complex dynamical behavior such as Hopf bifurcations or chaos, we perform a numerical bifurcation analysis. We fix all parameters except the delay parameters τ_1 and τ_2 (which appear in $\mathcal{R}_d$) and examine the long-term behavior of the system.

Figure 8 shows a bifurcation diagram of the infectious class I^* at equilibrium as a function of the total delay $\tau = \tau_1 + \tau_2$, with $\tau_1 = \tau_2 = \tau/2$. For $\tau_1 = \tau_2 = \tau/2$ and $n_1 = n_2 = 1$, the delayed reproduction number satisfies

$$R_d(\tau) = R_d(0)e^{-\tau}.$$

For the parameter set $\eta = 2.5$ and $\Lambda = 16$ used in the numerical experiment, $R_d(0) = 11.4583$. Hence the threshold total delay is $\tau_{\text{cr}} = \ln(11.4583) \approx 2.4387$. Thus, $R_d > 1$ for $\tau < 2.4387$ and $R_d \leq 1$ for $\tau \geq 2.4387$.

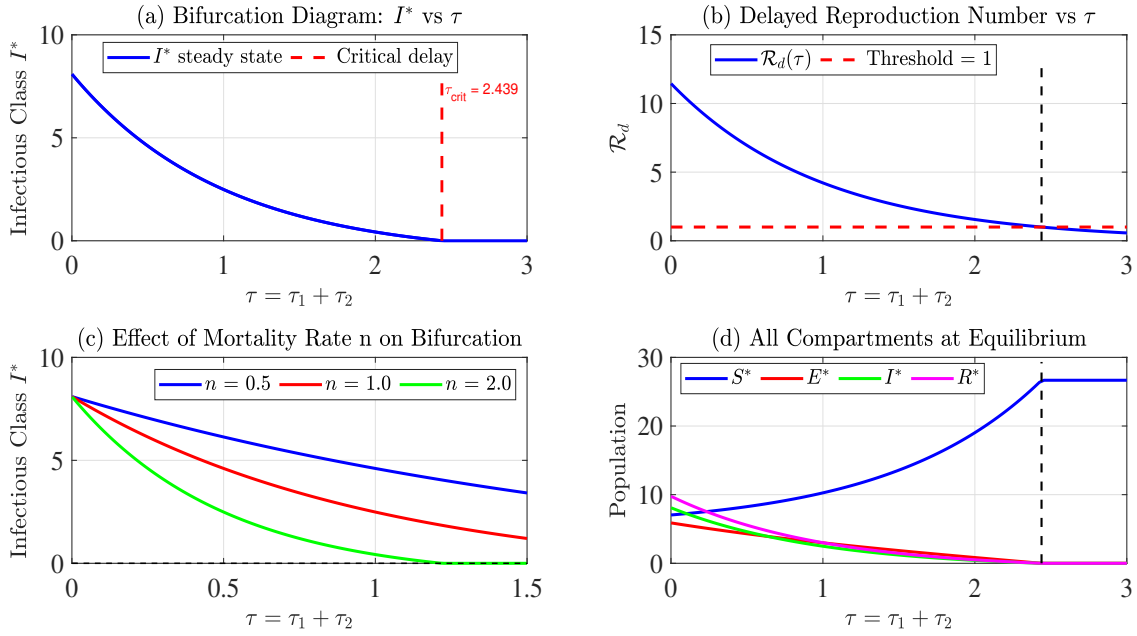


Figure 8. Bifurcation diagram of the infectious class I^* at equilibrium as a function of the total delay $\tau = \tau_1 + \tau_2$, with $\tau_1 = \tau_2 = \tau/2$.

As τ increases, the endemic equilibrium level decreases monotonically. No oscillatory behavior or Hopf bifurcations are observed for the parameter ranges considered. This monotonic behavior is consistent with the theoretical result that the delayed system exhibits global threshold dynamics: When $\mathcal{R}_d > 1$, the endemic equilibrium is globally asymptotically stable, and when $\mathcal{R}_d \leq 1$, the disease-free equilibrium is globally asymptotically stable. The delays affect the dynamics primarily through the reproduction number rather than by inducing complex dynamical behavior.

However, we note that the model's global stability results rely on the specific assumptions on the incidence function ψ (non-negative, increasing, and concave) and the delay kernels. For different functional forms or more complex delay structures, Hopf bifurcations or other dynamical phenomena could potentially arise. This remains an interesting direction for future investigation.

To further illustrate the impact of time delays on the transmission potential, Figure 9 shows the variation of the delayed basic reproduction number $\mathcal{R}_d$ as a function of the delay parameters τ_1 and τ_2. From the expression

$$\mathcal{R}_d = \frac{\epsilon\Lambda e^{-n_1\tau_1 - n_2\tau_2}\psi'(0)}{\mu_s(\mu_e + \epsilon)(\mu_i + \gamma)}, \tag{5.3}$$

we see that $\mathcal{R}_d$ decays exponentially with both τ_1 and τ_2. The decay rate is determined by the mortality rates n_1 and n_2 during the delay periods.

Panel (a) of Figure 9 shows the dependence of $\mathcal{R}_d$ on τ_1 for several values of n_1, with τ_2 fixed. Panel (b) shows the dependence on τ_2 for several values of n_2, with τ_1 fixed. Panel (c) shows a contour plot of $\mathcal{R}_d$ as a function of both τ_1 and τ_2.

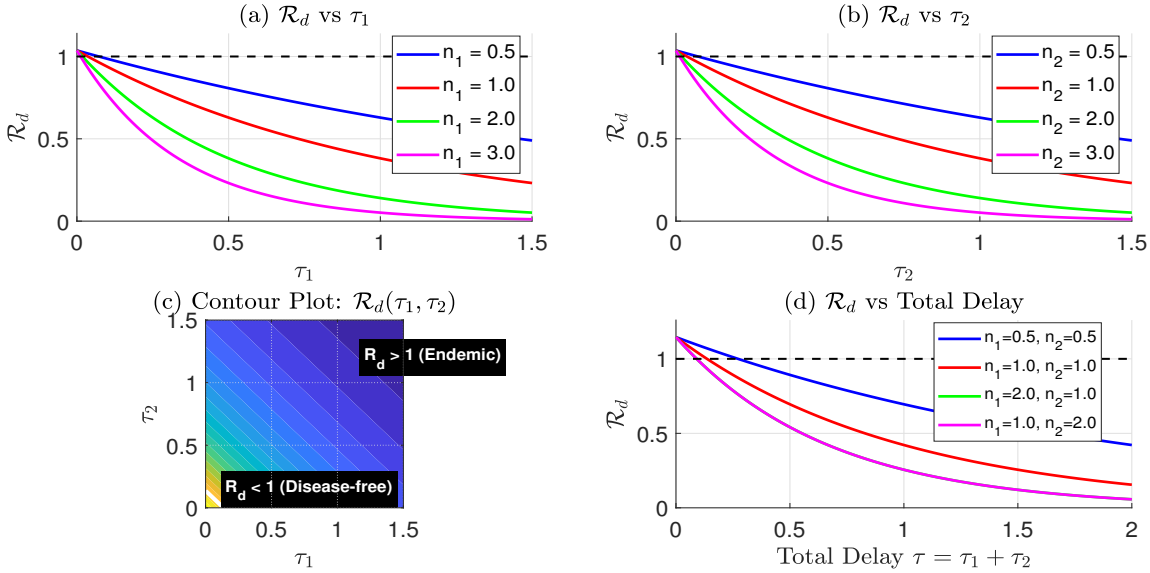


Figure 9. Variation of the delayed basic reproduction number $\mathcal{R}_d$ with respect to time delays. (a) $\mathcal{R}_d$ as a function of τ_1 for different values of n_1, with $\tau_2 = 0.1$ and $n_2 = 1$. (b) $\mathcal{R}_d$ as a function of τ_2 for different values of n_2, with $\tau_1 = 0.1$ and $n_1 = 1$. (c) Contour plot of $\mathcal{R}_d$ as a function of both τ_1 and τ_2 with $n_1 = n_2 = 1$.

These numerical results highlight that longer delays reduce the effective transmission potential because fewer infected birds survive long enough to become infectious or to transmit the virus. This effect is particularly important for avian influenza, where infected birds may die before progressing through the latent period. The results also show that the delay τ_3 (associated with recovery) does not affect $\mathcal{R}_d$, which is consistent with the analytical expression.

The strong dependence of $\mathcal{R}_d$ on the delays suggests that interventions that reduce the survival of infected birds during the latent period (e.g., through culling or biosecurity measures) can significantly reduce the transmission potential of avian influenza in bird populations.

6. Conclusions

This study developed an SEIR model for avian influenza transmission in a bird population with saturated incidence and distributed delays. The model follows birds through the susceptible, exposed, infectious, and recovered classes, while allowing the timing of infection progression and recovery to vary among birds. This structure reflects the biology of avian influenza more realistically, since infected birds may not become infectious or recover at the same rate.

First, we calculated the basic reproduction number, $\mathcal{R}_0$, for the non-delayed avian influenza model. Furthermore, we derived the delayed basic reproduction number, $\mathcal{R}_d$, for the distributed-delay model. The stability analysis shows that when the corresponding reproduction number is less than or equal to one, the disease-free equilibrium is globally asymptotically stable (see Theorems 3 and 5). In this case, avian influenza dies out in the bird population, and both the exposed and infectious classes approach zero. Conversely, when the reproduction number exceeds one, the disease persists, and the model admits a unique endemic equilibrium where susceptible, exposed, infectious, and recovered birds

coexist. It has been shown that this endemic equilibrium is locally and globally asymptotically stable (see Theorems 4 and 6), which means that positive solutions approach the endemic state whenever the threshold quantity is greater than unity. The numerical simulations support the theoretical findings and illustrate how distributed delays influence avian influenza persistence (see Figures 2–5).

A key contribution of this work is the rigorous distinction between local and global stability results for both the non-delayed and delayed systems. Local stability, established via eigenvalue and Routh-Hurwitz analyses, describes the asymptotic behavior of solutions near the equilibria. This is biologically interpreted as the system's response to small perturbations from the disease-free or endemic state. Global stability, established via Lyapunov functions for the non-delayed system and Lyapunov functionals for the delayed system, is a stronger result: It guarantees that all solutions, regardless of their initial conditions, converge to the corresponding equilibrium. Biologically, global stability of the disease-free equilibrium indicates that avian influenza will be eliminated from the bird population irrespective of how the infection is introduced, whereas global stability of the endemic equilibrium implies that the infection will persist and stabilize at a unique positive level under any initial exposure scenario. The transition from local to global stability analysis is particularly significant because it provides robust predictions that do not depend on the precise initial conditions of the outbreak.

The distributed-delay formulation further shows that delays affect disease invasion through survival-weighted factors. Longer delay periods or higher mortality during delayed stages reduce the probability that infected birds survive long enough to contribute to new infections, thereby decreasing $\mathcal{R}_d$ (see Figures 3 and 5).

A sensitivity analysis of $\mathcal{R}_d$ was also conducted. The results indicate that the recruitment of susceptible birds Λ is an essential element in $\mathcal{R}_d$. Simultaneously, susceptible-bird mortality μ_s, infectious-bird mortality μ_i, the recovery rate γ, and mortality during delayed stages are also critical in reducing $\mathcal{R}_d$. Biologically, this suggests that reducing contact among susceptible and infectious birds, limiting the introduction of new susceptible birds into infected settings, and rapidly detecting and removing infectious birds can substantially lower the risk of sustained transmission.

The infection-blocking control analysis further shows that reducing effective transmission can change the qualitative outcome of the system. As the control efficacy (p) increases, the controlled reproduction number ($\mathcal{R}_d^c(p)$) decreases, and once p exceeds the critical value, the infection-free equilibrium becomes stable. Biologically, this means that fewer susceptible birds are converted into the exposed class, leading to a decline in both exposed and infectious birds. The numerical results in Figure 7 support this behavior: Higher values of (p) increase the susceptible bird population while reducing the exposed, infectious, and recovered classes. In particular, when ($p = 0.95$), $\mathcal{R}_d^c(p)$ falls below one, and avian influenza is driven toward elimination. Thus, sufficiently strong transmission-blocking measures can shift the model dynamics from endemic persistence to disease extinction.

The proposed model has some limitations that should be considered. It treats the bird population as homogeneous and does not separate wild birds from domestic poultry, different age groups, or species. The model also does not explicitly account for environmental viral persistence, seasonal migration, spatial movement, or parameter estimation from observed data. Future work could extend the present framework by considering multiple interacting bird populations, particularly wild birds and domestic poultry. It would also be useful to include environmental contamination, seasonal forcing, and spatial movement.

Use of Generative-AI tools declaration

The author declares he has not used Artificial Intelligence (AI) tools in the creation of this article.

Acknowledgements

This work was funded by the University of Jeddah, Jeddah, Saudi Arabia, under grant No. (UJ-24-SUCH-711). The author, therefore, thanks the University of Jeddah for its technical and financial support. The author would also like to thank the anonymous referees and the editor for many constructive suggestions, which helped to improve the presentation of the paper.

Conflict of interest

The author declares no conflict of interest.

References

1. A. Blagodatski, K. Trutneva, O. Glazova, O. Mityaeva, L. Shevkova, E. Kegeles, et al., Avian influenza in wild birds and poultry: dissemination pathways, monitoring methods, and virus ecology, *Pathogens*, **10** (2021), 630. http://dx.doi.org/10.3390/pathogens10050630
2. World Organisation for Animal Health, Avian influenza, 2026. Available from: https://www.woah.org/en/disease/avian-influenza/.
3. A. Mena, M. E. von Fricken, B. D. Anderson, The impact of highly pathogenic avian influenza H5N1 in the United States: a scoping review of past detections and present outbreaks, *Viruses*, **17** (2025), 307. http://dx.doi.org/10.3390/v17030307
4. USDA Animal and Plant Health Inspection Service, Avian influenza, 2026. Available from: https://www.aphis.usda.gov/livestock-poultry-disease/avian/avian-influenza.
5. Centers for Disease Control and Prevention, About bird flu, 2024. Available from: https://www.cdc.gov/bird-flu/about/index.html.
6. Centers for Disease Control and Prevention, Current situation: bird flu in dairy cows, 2025. Available from: https://www.cdc.gov/bird-flu/situation-summary/mammals.html.
7. U. AbuBakar, L. Amrani, F. A. Kamarulzaman, S. A. Karsani, P. Hassandarvish, J. E. Khairat, Avian influenza virus tropism in humans, *Viruses*, **15** (2023), 833. http://dx.doi.org/10.3390/v15040833
8. World Organisation for Animal Health, Avian influenza vaccination: Why it should not be a barrier to safe trade, 2023. Available from: https://www.woah.org/app/uploads/2023/12/en-woah-policybrief-avianinfluenzavaccinationandtrade.pdf.
9. EFSA Panel on Animal Health and Animal Welfare, Vaccination of poultry against highly pathogenic avian influenza – part 1. Available vaccines and vaccination strategies, *EFSA J.*, **21** (2023), e8271. http://dx.doi.org/10.2903/j.efsa.2023.8271

10. USDA Animal and Plant Health Inspection Service, HPAI poultry innovation grand challenge, 2026. Available from: https://www.aphis.usda.gov/funding/highly-pathogenic-avian-influenza-hpai-poultry-innovation-grand-challenge.
11. Food and Agriculture Organization of the United Nations, Avian influenza, 2026. Available from: https://www.fao.org/animal-health/animal-diseases/avian-influenza/en.
12. S. Lambert, B. Bauzile, A. Mugnier, B. Durand, T. Vergne, M. C. Paul, A systematic review of mechanistic models used to study avian influenza virus transmission and control, *Vet. Res.*, **54** (2023), 96. http://dx.doi.org/10.1186/s13567-023-01219-0
13. P. S. Pandit, D. A. Bunn, S. A. Pande, S. S. Aly, Modeling highly pathogenic avian influenza transmission in wild birds and poultry in West Bengal, India, *Sci. Rep.*, **3** (2013), 2175. http://dx.doi.org/10.1038/srep02175
14. N. Tuncer, M. Martcheva, Modeling seasonality in avian influenza H5N1, *J. Biol. Syst.*, **21** (2013), 1340004. http://dx.doi.org/10.1142/S0218339013400044
15. T. Kang, Q. Zhang, H. Wang, Optimal control of an avian influenza model with multiple time delays in state and control variables, *Discrete Cont. Dyn. Syst. - Ser. B*, **26** (2021), 4147–4171. http://dx.doi.org/10.3934/dcdsb.2020278
16. World Organisation for Animal Health, *Chapter 3.3.4: Avian influenza, including infection with high pathogenicity avian influenza viruses*, In: *Manual of diagnostic tests and vaccines for terrestrial animals*, WOAH, Paris, 2021. Available from: https://www.woah.org/fileadmin/Home/eng/Health_standards/tahm/3.03.04_AI.pdf.
17. Merck Veterinary Manual, *Avian influenza in poultry and wild birds*, Merck & Co., Rahway, NJ, 2026. Available from: https://www.merckvetmanual.com/poultry/avian-influenza-in-poultry-and-wild-birds/avian-influenza-in-poultry-and-wild-birds.
18. H. H. Almuashi, M. El Hajji, Global dynamics of a dual-target HIV model with time delays and treatment implications, *Mathematics*, **14** (2026), 6. http://dx.doi.org/10.3390/math14010006
19. F. K. Alalhareth, A. A. Alharbi, M. H. Alharbi, M. El Hajji, Modeling Guinea worm disease with time delays: threshold dynamics, treatments and sensitivity analysis in heterogeneous populations, *AIMS Math.*, **11** (2026), 11116–11153. http://dx.doi.org/10.3934/math.2026458
20. M. El Hajji, Y. A. Al-Faidi, M. H. Alharbi, Modeling dual-colony Nosema transmission in honeybees: the role of distributed delays and antiviral treatment, *AIMS Math.*, **11** (2026), 2645–2681. http://dx.doi.org/10.3934/math.2026107
21. N. A. Almuallem, M. El Hajji, Global dynamics of a multi-population water pollutant model with distributed delays, *Mathematics*, **14** (2026), 20. http://dx.doi.org/10.3390/math14010020
22. O. Diekmann, J. A. P. Heesterbeek, J. A. J. Metz, On the definition and the computation of the basic reproduction ratio $\mathcal{R}_0$ in models for infectious diseases in heterogeneous populations, *J. Math. Biol.*, **28** (1990), 365–382. http://dx.doi.org/10.1007/BF00178324
23. P. van den Driessche, J. Watmough, Reproduction numbers and sub-threshold endemic equilibria for compartmental models of disease transmission, *Math. Biosci.*, **180** (2002), 29–48. http://dx.doi.org/10.1016/S0025-5564(02)00108-6

24. J. K. Hale, A. S. Somolinos, Competition for fluctuating nutrient, *J. Math. Biol.*, **18** (1983), 255–280. http://dx.doi.org/10.1007/BF00276091

25. H. K. Khalil, *Nonlinear systems*, 2 Eds., Prentice Hall, 1996.

26. J. P. LaSalle, *The stability of dynamical systems*, Philadelphia: Society for Industrial and Applied Mathematics, 1976. http://dx.doi.org/10.1137/1.9781611970432

27. A. M. Elaiw, E. A. Almohaimeed, A. D. Hobiny, Stability of HHV-8 and HIV-1 co-infection model with latent reservoirs and multiple distributed delays, *AIMS Math.*, **9** (2024), 19195–19239. http://dx.doi.org/10.3934/math.2024936

28. Y. N. Kyrychko, K. B. Blyuss, Global properties of a delayed SIR model with temporary immunity and nonlinear incidence rate, *Nonlinear Anal.: Real World Appl.*, **6** (2005), 495–507. http://dx.doi.org/10.1016/j.nonrwa.2004.10.001

29. S. A. Gourley, Y. Kuang, A delay reaction-diffusion model of the spread of bacteriophage infection, *SIAM J. Appl. Math.*, **65** (2004), 550–566. http://dx.doi.org/10.1137/S0036139903436613

30. N. Chitnis, J. M. Hyman, J. M. Cushing, Determining important parameters in the spread of malaria through the sensitivity analysis of a mathematical model, *Bull. Math. Biol.*, **70** (2008), 1272–1296. http://dx.doi.org/10.1007/s11538-008-9299-0

31. C. J. Silva, D. F. M. Torres, Optimal control for a tuberculosis model with reinfection and post-exposure interventions, *Math. Biosci.*, **244** (2013), 154–164. http://dx.doi.org/10.1016/j.mbs.2013.05.005

32. A. Sorokin, I. Goryanin, FBA-PRCC. Partial Rank Correlation Coefficient (PRCC) global sensitivity analysis (GSA) in application to constraint-based models, *Biomolecules*, **13** (2023), 500. http://dx.doi.org/10.3390/biom13030500

33. S. Marino, I. B. Hogue, C. J. Ray, D. E. Kirschner, A methodology for performing global uncertainty and sensitivity analysis in systems biology, *J. Theor. Biol.*, **254** (2008), 178–196. http://dx.doi.org/10.1016/j.jtbi.2008.04.011

34. S. M. Blower, H. Dowlatabadi, Sensitivity and uncertainty analysis of complex models of disease transmission: an HIV model, as an example, *Int. Stat. Rev.*, **62** (1994), 229–243. http://dx.doi.org/10.2307/1403510

35. W. J. Conover, *Practical nonparametric statistics*, 2 Eds., New York: John Wiley & Sons, 1980.



AIMS Press

© 2026 the Author(s), licensee AIMS Press. This is an open access article distributed under the terms of the Creative Commons Attribution License (http://creativecommons.org/licenses/by/4.0)